Specific reduction in complex I of the mitochondrial electron transport system in long-lived seed beetles

By

Heather Mast

A thesis submitted in partial fulfillment of the requirements for the degree of

Master of Science

Department of Medicine

University of Alberta

ABSTRACT

Background: Mitochondrial dysfunction is a recognized hallmark of aging that is also directly or indirectly connected to practically all the other hallmarks of aging. As a result, mitochondrial dysfunction seems to be an important regulator of lifespan. Many studies provide evidence of lifespan extension following a decrease in mitochondrial complexes, but few studies have actually measured and compared integrated mitochondrial function. Additionally, most studies on longevity are on a limited number of animal models, such as *Drosophila* and *Caenorhabditis elegans*.

Methods: Here, we measured integrated mitochondrial function in the seed beetle, *Acanthoscelides obtectus*. This animal model has been selected for early (E) and late (L) reproduction for nearly four decades and over 250 generations, leading to two lines of the same animal species, each with a very different longevity (7 days in E line, 12-14 days in L line). First, we determined mitochondrial content and used high-resolution respirometry to measure the NADH, Succinate, and Proline dehydrogenase pathways and complex IV in short-lived (E line) and long-lived (L line) beetles of both sexes and at 3 timepoints (days 1, 5, and 8). Second, we determined complex I, complex II, and complex IV's control over combined NADH+Succinate+Proline flux in male beetles at days 1 and 5. Lastly, we tested fatty acid oxidation.

Results: The NADH pathway's contribution to maximal flux was lower and the Succinate pathway's contribution was higher in L line beetles, mostly at days 1 and 5, suggesting a link between early differences in mitochondrial function and longevity. Control by complex I was also stronger and complex IV had a higher excess capacity in L line beetles at day 1 of age. Male beetles

tended to have more longevity-linked differences compared to females. There were no differences in proline and fatty acid metabolisms between the beetle selection lines.

Conclusion: The combined reduction in the NADH pathway and increased control of mitochondrial respiration by complex I suggest that complex I contributes to the lifespan extension seen in L line beetles. The opposite seems to be true for E line beetles. This work, comparing different selection lines within the same animal species, reinforces the involvement of mitochondrial dysfunction in lifespan while also evaluating sex differences and additional metabolic pathways.

PREFACE

This thesis is an original work by Heather Mast. No part of this thesis has been previously published. This research project is a collaboration with Drs. M. Đorđević and U. Savković (Institute for Biological Research "Siniša Stanković" National Institute of the Republic of Serbia, University of Belgrade, Belgrade, Serbia) and Dr. P.U. Blier (Département de Biologie, Université du Québec, Rimouski, Quebec, Canada).

ACKNOWLEDGMENTS

I would first like to thank my supervisor, Dr. Hélène Lemieux, for her never-ending support throughout my university academic career. Her knowledge and research experiences have been invaluable and always offer something new for me to learn. Thank you also to my co-supervisor, Dr. Pierre Blier, for his feedback and support throughout my program, and also for his generosity in allowing me the unforgettable opportunity to work in his lab in Rimouski in the summer of 2022. Thank you to Drs. Mirko Đorđević and Uroš Savković for their continued help with maintaining beetle populations and overall support. Huge thanks also to Dr. Stephane Bourque as a supervisory committee member, Dr. Sandra Davidge as my arms-length examiner, and Dr. Gavin Oudit as Chair. Finally, thank you to Claudia Holody for her assistance with some of the inhibitor titration experiments.

TABLE OF CONTENTS

LIST OF FIGURES

ABBREVIATIONS

CI	Complex I
CII	Complex II
CIII	Complex III
CIV	Complex IV
CS	Citrate synthase
ET	Electron transfer
ETF	Electron-transferring flavoprotein
ETS	Electron transport system
FAO	Fatty acid β-oxidation
FCR	Flux control ratio
IU	International units
NS	NADH+Succinate
NSPro	NADH+Succinate+Proline
OXPHOS	Oxidative phosphorylation
ProDH	Proline dehydrogenase
RNAi	RNA interference
ROS	Reactive oxygen species
ROX	Residual oxygen consumption
UPRmt	Mitochondrial unfolded protein response

1. INTRODUCTION

1.1 The hallmarks of aging

During the process of aging, animals face a progressive loss of physiological integrity, which is characterized by stochastic damages to tissues and cellular components, impairment of global and cellular functions, and an increased risk of various diseases such as cancer, diabetes, and neurodegenerative and cardiovascular disorders (Akbari et al., 2019; Kirkwood, 2005). Despite the considerable importance of aging in health, its mechanism still remains fairly unknown.

Nine key biological pathways that drive the aging process have been proposed and identified as the hallmarks of aging: mitochondrial dysfunction, genomic instability, telomere attrition, epigenetic alterations, loss of proteostasis, deregulated nutrient sensing, cellular senescence, stem cell exhaustion, and altered intercellular communication (López-Otín et al., 2013; López-Otín et al., 2016). More recently, a few more were added: compromised autophagy, microbiome disturbance, altered mechanical properties, dysregulation of RNA processing, and inflammation (Schmauck-Medina et al., 2022). Interestingly, mitochondrial dysfunction is classified as an antagonistic hallmark of aging, i.e., one that could have both beneficial effects at low levels and deleterious effects at higher levels (López-Otín et al., 2013). Another important aspect is that mitochondrial dysfunction can be linked directly or indirectly with most of, if not all, the other hallmarks of aging (Cai et al., 2022; Fakouri et al., 2019; Ferrucci et al., 2022; Li et al., 2022; Lu and Guo, 2020; Milani et al., 2022; Minocherhomji et al., 2012; Okamoto and Kondo-Okamoto, 2012; Phillip et al., 2015; Rehman et al., 2023; Schiavi and Ventura, 2014; Tomtheelnganbee et al., 2022; Torres and Perez, 2008; Wan and Finkel, 2020; Zheng et al., 2019) and to the diseases linked to aging, such as Parkinson's (van der Walt et al., 2003), type 2 diabetes (Ohkubo et al.,

2000), cardiovascular diseases (Lemieux et al., 2011) and Alzheimer's (Lakatos et al., 2010). This is not surprising, since mitochondria have multiple functions in cells, i.e., catabolism and energy production through the process of oxidative phosphorylation (OXPHOS), production and buffering of reactive oxygen species (ROS), regulation of cellular metabolism, anabolism, biosynthesis of iron-sulfur clusters and heme, homeostasis of calcium and iron, apoptosis, intracellular signaling, regulation of innate immunity, and modulation of stem cell activity (reviewed by Finkel, 2015; Srivastava, 2017; Sun et al., 2016).

All of this places mitochondria as a central point in the intense and complex mechanism of aging, the diseases associated to aging, and ultimately the regulation of lifespan (Akbari et al., 2019; Balaban et al., 2005; Klaus and Ost, 2020; Long et al., 2014; López-Otín et al., 2013; Mattson and Arumugam, 2018; Sun et al., 2016). Regulating lifespan not only aims at increasing the time an individual lives, but also at increasing an individual's healthspan by preserving bodily functions and delaying the development of aging-related diseases.

1.2 Reactive oxygen species production and aging

Over the years, many proposed theories of aging have incorporated mitochondria directly and/or indirectly. One of these, the "Free Radical Theory of Aging" (Harman, 1956), connected the production of highly reactive oxygen species (e.g., hydroxyl radical, a by-product of normal metabolism) to the damage of cellular macromolecules, like DNA, lipids, and proteins. Harman then elucidated that mitochondria produced the most important amount of ROS due to their use of oxygen through the OXPHOS process. As a result, the first molecules attacked by ROS are on site, i.e., mitochondrial DNA, mitochondrial proteins such as those part of the electron transport system

(ETS), and phospholipids of the internal and external mitochondrial membranes. This then became a unifying hypothesis known as the "Mitochondrial Free Radical Theory of Aging" (Harman, 1972).

Strong criticism to the Mitochondrial Free Radical Theory of Aging questions the role (if any) of ROS – and consequently of antioxidants – in the aging process (Blier et al., 2017; Hekimi et al., 2011; Stuart et al., 2014). This criticism is based, among others, on the following: (1) the levels of antioxidant molecules and enzymes, aimed at eliminating ROS, do not positively correlate with animal longevity (Buffenstein et al., 2008; Hekimi et al., 2011; Pérez et al., 2009; Stuart et al., 2014) , (2) lifelong antioxidant supplementation studies have failed to extend lifespan and, in some cases, antioxidant micronutrients even accelerated the aging process (Stuart et al., 2014), (3) evidence does not support that ROS production shortens life span (Ballard et al., 2007; Copeland et al., 2009; Munro et al., 2013; Van Raamsdonk and Hekimi, 2009; Yang et al., 2007), (4) the increase in lifespan in *Caenorhabditis elegans* with compromised mitochondria due to RNA interference (RNAi) is not associated with a change in free radical production (Lee et al., 2003), (6) administration of pro-oxidant molecules prolonged lifespan in *C. elegans* (Schaar et al., 2015), and (7) even with the known important contribution of complex I (CI) to ROS production, some studies correlating the low level of CI function with extended longevity have shown that the regulatory role of CI can be uncoupled from ROS production (Bratic and Trifunovic, 2010; Copeland et al., 2009; Lambert et al., 2010; Pujol et al., 2013).

So, the link between mitochondria and aging is not necessarily dependent on mitochondrial ROS production, and is far more complex than originally perceived. In fact, ROS, at moderate levels, can not only be damaging molecules, but can also be used as critical signaling molecules. This has led to the development of a concept called mitohormesis, i.e., when signaling molecules cause an

adaptive response that enhances not only cellular stress resistance and systemic defense, but also life expectancy (reviewed by Ristow and Schmeisser, 2014; Ristow and Zarse, 2010; Son and Lee, 2019; Srivastava, 2017; Yun and Finkel, 2014).

1.3 Changes in mitochondrial OXPHOS during aging

One important step in understanding the role of mitochondria in aging is to understand how mitochondrial function, and in particular OXPHOS, is affected during the aging process. In eukaryotic cells, mitochondria produce a large proportion of energy using the OXPHOS process, composed of the ETS and the phosphorylation system (includes ATP synthase, the phosphate carrier, and adenine nucleotide translocase, ANT). Electrons from NADH enter the ETS through CI, then pass through the Q-junction, complex III (CIII), cytochrome *c*, and complex IV (CIV). Electrons from succinate enter the ETS through complex II (CII) and are then transferred to the Q-junction, CIII, cytochrome *c*, and CIV. Additional electron entries also meet at the Q-junction (Fig. 1), such as the Proline dehydrogenase (ProDH) pathway (electrons from proline), the Electron-transferring flavoprotein (ETF) pathway (electrons from various fatty acids), the Glycerophosphate dehydrogenase pathway (electrons from glycerophosphate), the Dihydroorotate dehydrogenase pathway (electrons from dihydroorotate), and the Sulfide:quinone oxidoreductase pathway (electrons from hydrogen sulfide; reviewed by Lemieux and Blier, 2022). All of these electrons are ultimately accepted by oxygen at CIV. While the electrons are being transferred, a proton gradient is created by CI, CIII, and CIV, which pump protons outside the intermembrane. ATP synthase utilizes this proton gradient to phosphorylate ADP into the cellular energy currency,

ATP. Phosphate and ADP are transported into mitochondria using the phosphate carrier and the ANT.

When the body ages, there are changes that occur in the OXPHOS process. Several studies have shown a decrease in mitochondrial function during aging in nearly all tissues, especially those demanding high energy, such as the heart, skeletal muscle, brain, liver, and in whole animals of small invertebrates.

In the rat heart, mitochondrial defects associated with aging have been localized at CIII (Lesnefsky et al., 2001; Lesnefsky et al., 2006) and CIV (Fannin et al., 1999; Lemieux et al., 2010; Lesnefsky et al., 2006; Paradies et al., 1993; Paradies et al., 1994; Paradies et al., 1997), specifically in the interfibrillar mitochondrial population (Fannin et al., 1999; Hoppel et al., 2017). Fatty acid β-oxidation (FAO), which provides a very important proportion of energy for the heart, has also been reported as defective in aged heart mitochondria (Hansford, 1978).

In skeletal muscle from aged rats and humans, a reduction in muscle mass (sarcopenia; Morley et al., 2001) and performance (Lanza et al., 2005; Lee et al., 1998) occurs. Mitochondrial performance in aged skeletal muscle, however, has also been demonstrated to be unaffected, as shown by similar rates of OXPHOS with different substrates in young and old rats (Beyer et al., 1984; Kerner et al., 2001) and in humans (Barrientos et al., 1996; Rasmussen et al., 2003a; Rasmussen et al., 2003b). But, there are also contrasting results for skeletal muscle mitochondria in the literature, as a decrease in OXPHOS in the presence of substrates feeding electrons into CI or CII has been reported in skeletal muscle from aged mice (Figueiredo et al., 2009) and humans (Tonkonogi et al., 2003), as well as a decrease in activities of CI (Choksi et al., 2008; Mansouri et al., 2006; Sugiyama et al., 1993), CII (Choksi et al., 2008), CIII (Choksi et al., 2008), CIV

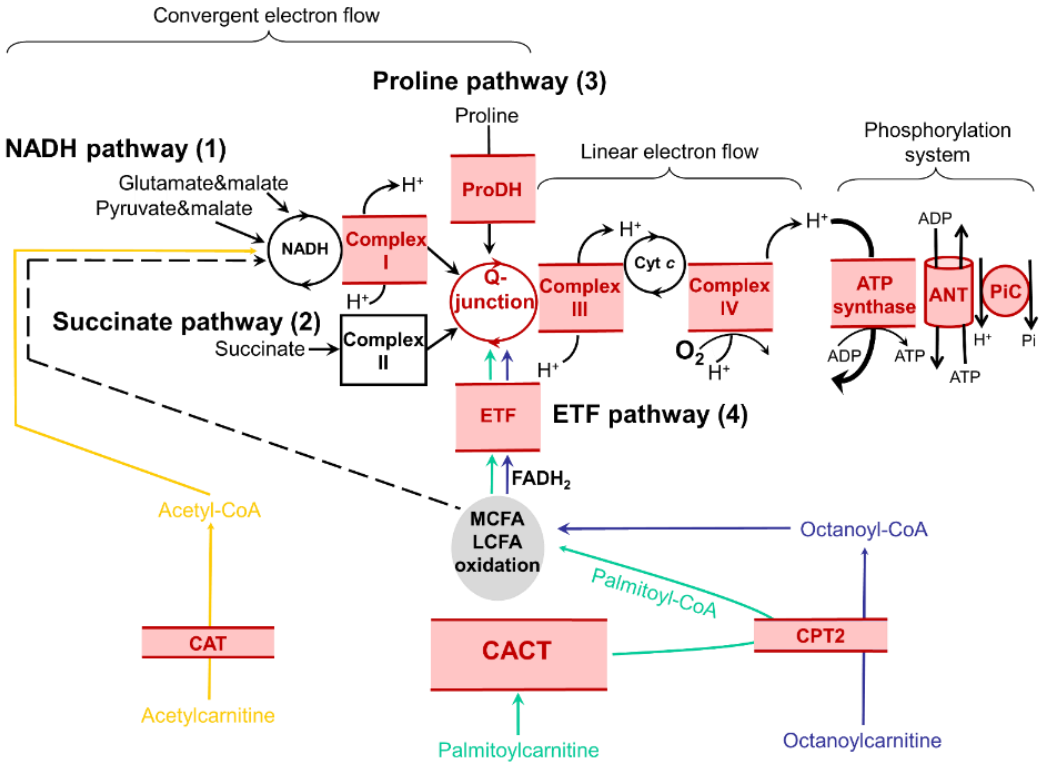

Figure 1: Electron entrances into oxidative phosphorylation (OXPHOS). This figure represents the four entries (described as number 1 to 4) tested in the current study, which converge at the Q-junction (ubiquinol/ubiquinone) of the OXPHOS system. **(1)** The NADH pathway provides electrons to complex I of the electron transport system. These electrons are provided here by malate, pyruvate, and glutamate. **(2)** The Succinate pathway through complex II uses succinate dehydrogenase to reduce FAD while converting succinate to fumarate. **(3)** Proline dehydrogenase (ProDH) catalyzes proline oxidation and FAD reduction. **(4)** The Electron-transferring flavoprotein (ETF; located on the matrix side of the inner mitochondrial membrane) pathway receives electrons from $FADH_2$, which is the product of fatty acid oxidation of various chain lengths of fatty acyl-CoA. When the long-chain fatty acid (LCFA) palmitoylcarnitine is the available substrate (path illustrated in green), it passes through the inner mitochondrial membrane using carnitine-acylcarnitine translocase (CACT); carnitine palmitoyltransferase 2 (CPT2) converts it to palmitoyl-CoA, then it enters the process of LCFA oxidation which reduces FAD to $FADH_2$. When the medium-chain fatty acid (MCFA) octanoylcarnitine is provided as the substrate (path illustrated in purple), it is converted to octanoyl-CoA by CPT2 and then follows the specific path for MCFA oxidation. The dashed line linking LCFA and MCFA oxidation to the NADH pathway indicates that NADH is generated in one step of fatty acid oxidation but acts as a minor and non-rate-limiting step in this pathway. When the short-chain fatty acid acetylcarnitine is used as a substrate (path illustrated in yellow), it passes directly through carnitine acetyltransferase (CAT) and enters the citric acid cycle, providing NADH for the NADH pathway. Malate is also provided as a substrate with all fatty acids, as it prevents accumulation of acetyl-CoA and concurrent inhibition of fatty acid oxidation. After convergence of electrons from diverse pathways at the Q-junction, they follow a linear segment through complexes III and IV before reducing molecular oxygen. Electron transfer is coupled with proton pumping into the intermembrane space by complexes I, III, and IV, generating a proton motive force providing the energy required to phosphorylate ADP into ATP by ATP synthase (part of the phosphorylation system is also supported by adenine nucleotide translocase [ANT] and the phosphate carrier [PiC]). All components shown here are located in or are peripherally associated with the inner mitochondrial membrane; transmembrane components are in red, and peripheral components are in black (i.e., complex II). Modified from Lemieux and Blier (2022); Mast et al. (2022).

(Choksi et al., 2008; Sugiyama et al., 1993; Tonkonogi et al., 2003), and ATP synthase (Choksi et al., 2008; Mansouri et al., 2006). Furthermore, the content of several mitochondrial proteins has been shown to be reduced in older mouse muscle (Short et al., 2005).

In the brain, mitochondrial mass did not vary with age (Navarro and Boveris, 2004), but OXPHOS with CI- and CII-linked substrates was lower in aged compared to young rats (Cocco et al., 2005), as well as the activities of CI (Boveris and Navarro, 2008; Cocco et al., 2005; Navarro et al., 2008; Navarro et al., 2007), CI+CIII (Navarro and Boveris, 2004; Navarro et al., 2004), and CIV (Boveris and Navarro, 2008; Haripriya et al., 2004; Itoh et al., 1996; Navarro and Boveris, 2004; Navarro et al., 2004; Navarro et al., 2008; Navarro et al., 2007; Ojaimi et al., 1999; Tian et al., 1998).

In the liver of aged compared to young rodents, mitochondrial mass was preserved (Navarro and Boveris, 2004), but there was a decrease in mitochondrial OXPHOS in the presence of substrates feeding electrons into CI, CII, or CIII (Castelluccio et al., 1994; Darnold et al., 1990; Genova et al., 1995; Okatani et al., 2002; Vazquez and Hoppel, 2004; Vazquez and Hoppel, 2005). Because the activities of CII (Navarro et al., 2007; Vazquez and Hoppel, 2004; Vazquez and Hoppel, 2005), CII+CIII (Navarro and Boveris, 2004), and CIV (Vazquez and Hoppel, 2004; Vazquez and Hoppel, 2005) were unaltered by age in rat liver, it was suggested that the decrease in OXPHOS was explained by a defect in CI or CIII. An additional defect in CIV activities was observed in the liver of aged mice (Navarro and Boveris, 2004; Navarro et al., 2004; Navarro et al., 2007).

Aging has also been associated with many OXPHOS changes in ectothermic animal models, including invertebrate species. With the wide range of invertebrate species, the diversity could bring new insight to the variation in aging mechanisms, providing valuable information that could lead to breakthroughs in mammal research. There are some commonly used invertebrates in aging

research, such as *Drosophila* and *C. elegans*. Studies have shown a decrease in CIV activity with age in *D. simulans* (Melvin and Ballard, 2006) and in *D. melanogaster* (Ferguson et al., 2005). In *C. elegans*, there was a reduction in CI with age (Yasuda et al., 2006). Additionally, a reduction in O_2 flux (Gruber et al., 2011; Yasuda et al., 2006) and overall ATP production in *C. elegans* has been observed with age (Gruber et al., 2011). Other animal models have also had changes in OXPHOS with age, such as a decrease in CI, CIV, and ATP synthase activities in honey bees (Alaux et al., 2009). Again, the varying involvement of OXPHOS with age between study organisms emphasizes the need to increase the species studied, in order to understand the differences between species and possible explanations for these differences.

1.4 Can changes in mitochondrial function control longevity?

Since mitochondrial dysfunction has been connected to aging, researchers are now questioning if it is possible to increase longevity and healthspan by modifying mitochondrial function, and if so, how would mitochondrial function need to be affected (increase or decrease), on which specific mitochondrial components, and at which phase in life would these mitochondrial changes need to occur. The literature seems to support that changes in mitochondrial activity can activate pathways leading to lifespan extension. A study performed on *C. elegans* showed an increase in longevity through partial inhibition of specific ETS components with inhibitors of CI (rotenone) and CIII (antimycin A; Labbadia et al., 2017). In a study on killifish, after noticing that a lower CI activity was associated with a longer lifespan, the team applied long-term pharmacological inhibition of CI with rotenone and succeeded to increase lifespan by 15% (Baumgart et al., 2016). The method of RNAi in *C. elegans* has also been shown to be positively associated with lifespan extension

when reducing CI and III (Yang and Hekimi, 2010b), CI, CIII, CIV, and ATP synthase (Dillin et al., 2002; Hansen et al., 2005; Rea et al., 2007), CI (Rauthan et al., 2015), CI and ATP synthase (Curran and Ruvkun, 2007), CI, CIV, and ATP synthase (Hamilton et al., 2005), CI, CIII, and CIV (Labbadia et al., 2017), and ATP synthase (Xu et al., 2018). The same phenomenon has been observed in *Drosophila* after applying RNAi for the genes corresponding to CI (Owusu-Ansah et al., 2013) and CI, CIII, CIV, and ATP synthase (Copeland et al., 2009). In *C. elegans*, a knockdown of the nuclear-encoded CIV-1 subunit Vb/COX4 (*cco-1*) in the intestine and the nervous system (Durieux et al., 2011), a mutation of the iron sulfur protein (*isp-1*) of CIII (Feng et al., 2001), and an altered mitochondrial condition in young animals by *Mclk1* (involved in ubiquinone biosynthesis) knockdown (Lapointe et al., 2009) all resulted in an increased longevity. In mice, a prolongation of lifespan has been observed after a mutation of the *Surf1* gene, a gene encoding a putative CIV assembly factor (Dell'agnello et al., 2007). Proline metabolism has additionally been shown to be involved in lifespan. In the yeast *Saccharomyces cerevisiae*, intracellular (Mukai et al., 2019) and extracellular (Nishimura et al., 2021) proline contributed to a longer lifespan. Proline metabolism was also involved in the longevity of *C. elegans*, since defective proline metabolism shortened lifespan (Pang and Curran, 2014) and supplemental proline extended lifespan (Edwards et al., 2015). Interestingly, no success in lifespan extension was obtained by decreasing CII function in *C. elegans* (Hamilton et al., 2005; Kuang and Ebert, 2012; Yang and Hekimi, 2010b). As the activity of mitochondrial complexes or specific steps involved in the OXPHOS process were not measured in most of these studies, it is difficult to know how much change in mitochondrial function was needed to obtain lifespan extension, and at which specific life-stage of the animal mitochondrial changes produced the largest effect.

There are also observations of mitochondrial dysfunction indirectly altering lifespan: (1) mutations

of the *clk-1* gene in *C. elegans*, a gene controlling mitochondrial respiration, resulted in lifespan extension (Lakowski and Hekimi, 1996; Wong et al., 1995); (2) knockdown of the conserved heat shock factor binding protein (HSB-1) resulted in increased histone H4 levels early in development, which altered the chromatin state of mtDNA, decreased expression of mtDNA-encoded genes, reduced mitochondrial respiratory capacity (not measured for specific complexes), and promoted lifespan extension (Sural et al., 2020); (3) a loss of mitochondrial DNA led to a loss of mitochondrial function and an increased lifespan in *S. cerevisiae* (Kirchman et al., 1999), but this observation is anticipated in this species since *S. cerevisiae* depends primarily on fermentation as an energy source.

Some data support the opposite relationship between mitochondrial dysfunction and lifespan, i.e., the loss of mitochondrial function associated with a shorter lifespan. First, various mutations compromising mitochondrial functionality in humans led to life-shortening diseases (Bénit et al., 2004; Campuzano et al., 1996; Graham et al., 1997; Wallace, 2005). In mice with a mutated gene for CI subunit 2, the defect on CI function occurred throughout life and provoked a shortening in lifespan (Hirose et al., 2019). In *Drosophila*, the inhibition of individual mitochondrial subunits from CI and CIV reduced the lifespan extension obtained with dietary restriction (Zid et al., 2009). In *C. elegans* as well, lifelong mutations that disrupt CI (*gas-1(fc21)*) and CII (*mev-1(kn1)*) have both been shown to produce a life-shortening effect (Ishii et al., 1990; Kayser et al., 2004). In *D. melanogaster*, a high fat diet was associated with a loss of respiration in the NADH pathway through CI and to faster aging (Cormier et al., 2019). In *Drosophila*, a mutation in the ND2 gene, which slightly reduced CI activity, was associated with a shorter lifespan (Burman et al., 2014; Wang et al., 2016). In *Daphnia pulex*, reduced CI activity was thought to contribute to their shorter lifespan (Ukhueduan et al., 2022). In *C. elegans*, reduced CI stability was associated with a

decrease in mitochondrial function, an increase in mitochondrial stress, and a shortened lifespan (Pujol et al., 2013). Similarly in human cells, less efficient CI assembly was associated with an increase in ROS production and produced premature senescence, whereas in mice, enhanced longevity was attained with complete CI assembly, since it improved the efficacy of substrate utilization by mitochondria and produced minimal ROS (Miwa et al., 2014).

To possibly explain the contrasts in the literature, it seems that negative changes in mitochondrial function aimed at increasing lifespan need to be of low magnitude, need to be linked to specific mitochondrial components, and/or need to occur within a specific phase in the life of the animal (which may vary between species). First, the increase in lifespan can be associated with negative changes in mitochondrial function, and can be reversed at a higher inhibition of the same mitochondrial function. In killifish, a dose of 0.5% rotenone increased lifespan, whereas a dose of 1% rotenone gave a strong reverse effect (Baumgart et al., 2016). In the seed beetle, a low concentration of 0.5% of the CI inhibitor tebufenpyrad maintained or slightly increased longevity, but higher concentrations of 1.5% or more decreased longevity (Jovanović et al., 2014). Second, only specific complexes and/or components of mitochondria can be targeted to produce lifespan extension. In *C. elegans*, where a decrease in CI, CIII, CIV, and ATP synthase showed an increase in lifespan (see above), a CII defect was unsuccessful in producing the same effect (Hamilton et al., 2005; Kuang and Ebert, 2012; Yang and Hekimi, 2010b). Lastly, the phase in life of the animal can influence the effect of mitochondrial changes on longevity. In *C. elegans*, the negative mitochondrial changes with positive effects on lifespan needed to occur in the L3/early L4 larval state (Dillin et al., 2002; Rea et al., 2007) or at the larval L1-L3 stage (Labbadia et al., 2017); a reduction of the ETS longevity pathway during adulthood did not result in an increased longevity (Dillin et al., 2002; Rea et al., 2007). These larval states in *C. elegans* could be linked to the effect

on longevity since the L4 stage is when the last somatic cell divisions occur in *C. elegans* (Rea et al., 2007). However, in the killifish, long-term pharmacological inhibition of CI with rotenone, starting at 23 weeks of age, succeeded to increase lifespan (Baumgart et al., 2016). From this contrast to results observed in various species, it seems probable that negative changes in mitochondrial function in the animal's life can positively influence lifespan, but the phase of life with the greatest potential for lifespan extension possibly varies between species. Of note, a large part of the data that shows the association between a decrease in mitochondrial function and lifespan were studied in *C. elegans*, with sporadic data collected on other species.

1.5 Our experimental model

To evaluate the changes in mitochondrial function with age and longevity, we used an experimental evolutionary approach with a seed beetle (*Acanthoscelides obtectus*) model developed in Serbia. This insect is a common pest of stored, dried legumes, so their natural environment can be easily mimicked in the lab. Selection from a base population for early (E line) and late (L line) reproduction began over 37 years ago (since 1986), affecting by default the mean longevity of the lines and the shape of their survival curves (Stojković and Savković, 2011; Tucić et al., 1996). Previous studies have shown that beetles from the L line now age about half as rapidly and live for about twice as long as beetles from the E line (i.e., 12-14 days for the L line and 7 days for the E line in mated individuals; (Đorđević et al., 2015) and are larger in size (Seslija et al., 2009). These differences apply to both sexes and reproductive states (i.e., virgin and mated; Đorđević et al., 2015; Đorđević et al., 2017; Stojković and Savković, 2011; Stojkovic et al., 2010).

This invertebrate model presents various advantages. First, it grants us the unique opportunity to measure, after decades of population selection, the key mitochondrial characteristics associated with changes in longevity. During evolution of a population, new characteristics or phenotypes may offer a longer potential lifespan when, for example, attributes that previously limited lifespan are overcome (Blier et al., 2017). And so, comparative animal models resulting from long-term evolution towards large differences in longevity can have the advantage of determining these new characteristics. This advantage of comparative animal models can most easily, if not exclusively, be found in ectotherms. Second, because of the short lifespan of the species, the changes can be compared cross-sectionally and longitudinally to determine not only which parameters but which time points in life are linked to these changes in longevity. Third, there is the option of seeing if the changes in mitochondrial function associated with longevity are linked with the sexes (male and female), contrasting with species such as *C. elegans* (males and hermaphrodites) where it is not possible. Fourth, we can better control the environmental, developmental, and nutritional conditions compared to other animal models since the beetles all develop within the same species of bean and adults are aphagous. And fifth, the comparisons between selection lines, ages, and sexes can be accomplished in a cost- and time-effective manner due to the low cost of maintaining the species.

Previous experiments led us to suspect the presence of metabolic differences between the E and L lines of *A. obtectus*. First, beetles from the L line showed a lower global metabolic rate compared to the E line (Arnqvist et al., 2017). Furthermore, important differences in metabolite content were also measured between these selection lines, with the L line showing a lower protein content and higher carbohydrate and lipid content compared to the E line, and marked changes related to sexes (Lazarevic et al., 2012). The lower metabolic rate in the L line agrees with the almost century old

observation showing that animals living at a faster metabolic rate also lived shorter lives, if the total energy expenditure was constant. This is known as the "rate of living" hypothesis (Pearl, 1928). Furthermore, differences in the mitochondrial ETS enzyme activities were determined. L line beetles mainly had an increase in CIII activity compared to the E line (Đorđević et al., 2017), but these differences were measured only at one time point at the beginning of the animal's life (day 1). Furthermore, despite giving valuable information on the capacity of some complexes, enzyme activity assays have important limitations when it comes to evaluating the global capacity of the OXPHOS process in physiological conditions. In contrast, with a polarographic assay, the measurement of integrated function is performed in live mitochondria, with intact ETS', and with the ETS components working together (Lemieux and Hoppel, 2009). This has never been performed on this animal model. And finally, another insight suggesting the use of more integrated methods to measure mitochondrial function between the selection lines is the result of a study administering a low dose of tebufenpyrad, an inhibitor of CI. When administered at day two and for 24 h, tebufenpyrad succeeded to increase longevity but only in males and only in the base population and the E line, whereas the opposite effect was observed in the L line (Jovanović et al., 2014). With these results in mind, measuring the integrated function of mitochondria enables us to better understand how specific metabolic pathways, and not just the activities of complexes, can be associated with longevity in the seed beetle model.

1.6 Objectives

The main objectives of this study were to determine how changes in mitochondrial function are linked with age and longevity using the seed beetle model presented in the section above. In order to accomplish this, we measured in the E and L beetle selection lines and at various time points during their life:

1) The integrated mitochondrial function using the technique of high-resolution respirometry (Oxygraph-2k OROBOROS Instruments Inc., Innsbruck, Austria) involving several specific pathways and complexes involved in the OXPHOS process (i.e., the NADH pathway, the Succinate pathway, the ProDH pathway (proline being an amino acid recognized as an energy source in insect flight muscle; Teulier et al., 2016), and the ETF pathway acting under various fatty acids with specific chain length, and CIV [see details in Fig. 1]).

2) The control by various complexes (CI, CII, CIV) using inhibitor titrations, as previously described (Lemieux et al., 2017; Rodríguez et al., 2021), as this control has also been shown to be linked with longevity in marine bivalves having strong variations in lifespan (Rodríguez et al., 2021).

3) The citrate synthase (CS) activity as a recognized marker of mitochondrial content (Larsen et al., 2012).

2. METHODS

2.1 Animal care

A. obtectus (Coleoptera: Bruchidae) were kept on organic, dry, common white beans (*Phaseolus vulgaris*) in dark incubators (Fisherbrand Isotemp, Fisher Scientific, Ottawa, ON, Canada) set at 30°C. Prior to use, beans were frozen and then brought to room temperature. Females lay eggs on or near beans, and first instar larvae bore inside. The complete larval development and pupation occurs inside beans. The final instar larvae excavate a chamber just below the bean testa. Pupation occurs in this chamber. Adults emerge one or two days after eclosion from their pupal case by chewing a hole through the bean testa. Upon hatching, beetles are moved to a new container with new beans on which to lay eggs. Adults are aphagous so need neither food nor water to reproduce. Females emerge with adequate energy to develop and lay most of their potential eggs (Tucić et al., 1996; Tucić et al., 1997).

2.2 Experimental populations

The two beetle lines were developed in Belgrade, Serbia from a base population by selecting the seed beetles for early (E) reproduction or late (L) reproduction for over 250 generations since 1986 (Tucić et al., 1996; Tucić et al., 1997). Beetles of the E line are permitted to lay eggs within the first 48 hours after emerging from *P. vulgaris*. After these 48 hours, beetles are removed. Beetles of the L line are permitted to lay eggs beginning from the 10^{th} day after emerging from *P. vulgaris* and are allowed to lay eggs until their death (for the selection process, see Tucić et al., 1996; Tucić et al., 1997).

2.3 Tissue preparation for respiratory measurements

Four replicates for each selection regime were used in the current study for each of the E and L lines. Beetles aged 1, 5, and 8 days old post-eclosion were collected. These timepoints include one early in life (day 1) and one at the end of life (day 8) for our short-lived E line. Day 5 was chosen as a middle timepoint. Each beetle's sex was identified by the dorsal colour and pattern of their butt; females have a white and brown checkerboard pattern on their butts, whereas males have solid brown butts. Each beetle was placed in a 4℃ fridge for 5-10 minutes to facilitate weight measurement by stopping beetle movement. After collecting its body weight, using a Mettler Toledo XS205 analytical balance, individual, whole beetles were immediately put in 3 mL of ice-cold Mitochondrial Respiration Medium 05 (MiR05; 0.5 mM EGTA, 3 mM MgCl2-6H2O, 60 mM K-lactobionate, 20 mM taurine, 10 mM KH2PO4, 20 mM HEPES, 110 mM sucrose, and 1 g/L BSA essentially fatty-acid free, pH 7.1; Gnaiger et al., 2000). Tissue homogenates were gently prepared on ice using a Potter-Elvehjem device connected to an overhead stirrer (Wheaton Instruments, Millville, NJ, USA) at a speed of 0.8 for 5 ± 2 passes as needed.

2.4 Measurements of NADH, Proline, and Succinate pathway capacities as well as complex IV activity using high-resolution respirometry

Immediately after preparation of the tissue homogenate, mitochondrial respiration was measured at 30℃ using an Oroboros Oxygraph-2k (OROBOROS Instruments Inc., Innsbruck, Austria). Chambers were previously calibrated with 2 mL of MiR05.

The protocol used included two respiratory states: LEAK (non-phosphorylation in the absence of

ADP) and OXPHOS (coupled phosphorylation of ADP in the presence of saturating ADP). Preliminary assays determined the appropriate homogenization technique that displayed the optimal rate of respiration, coupling preservation (low LEAK state compared to the OXPHOS state), as well as mitochondrial outer membrane integrity (lower effect of exogenous cytochrome *c*). Tests also confirmed no limitation of OXPHOS capacity by the phosphorylation system (ATP synthase, ADP/ATP transport, or the phosphate carrier) because the oxygen consumption following addition of DNP as an uncoupler did not increase. As a result, respiration in the OXPHOS state and electron transfer (ET) capacity were considered equivalent.

From each chamber, after calibration, a volume of 0.5 mL of MiR05 was removed. Then, we added pyruvate (5 mM), malate (5 mM), glutamate (10 mM) and 0.5 mL of each tissue homogenate for a final chamber volume of 2 mL. The chamber was then closed to determine the LEAK state. Then, the following substrates and inhibitors were added: 2.5 mM ADP (OXPHOS state through the NADH pathway via CI), 10 µM cytochrome *c* (outer mitochondrial membrane integrity test), 10 mM succinate (OXPHOS state for the combined NADH and Succinate pathways, the NS pathway), 10 mM L-proline (OXPHOS state for the combined NS pathways and ProDH pathway, the NSPro pathway), 1 µM rotenone (OXPHOS state through the Succinate pathway via CII and part of the ProDH pathway), 5 µM antimycin A (non-mitochondrial residual oxygen consumption, ROX), 2 mM ascorbate and 0.5 mM N,N,N',N'-tetramethyl-p-phenylenediamine (TMPD; CIV activity), and 100 mM sodium azide (chemical background). Mitochondrial respiration was measured in pmol O_2 per second per mg of tissue and corrected for ROX, except for CIV which was corrected for the chemical background.

FAO was additionally measured in tissue homogenates of male beetles at day 1 by adding either 0.02 mM palmitoylcarnitine and 5 mM malate, 0.2 mM octanoylcarnitine and 5 mM malate, or 2.5

mM acetylcarnitine and 5 mM malate as the initial substrates, followed by 2.5 mM ADP, 10 µM cytochrome *c*, 5 mM pyruvate and 10 mM glutamate, 10 mM succinate, 10 mM L-proline, and 100 mM sodium azide.

2.5 Control of mitochondrial respiratory capacity using high-resolution respirometry

Additional sets of high-resolution respirometry experiments were conducted to identify the control by specific complexes, i.e., CI within the NADH pathway, CII within the Succinate pathway, and CIV, as previously described (Lemieux et al., 2017; Rodríguez et al., 2021). Both chambers of each oxygraph were given the same quantity of homogenate from the same animal. For measuring the control of each complex, one chamber (i.e., chamber A) measured the maximal global capacity with all measured pathways active (with pyruvate, glutamate, malate, ADP, cytochrome *c*, succinate, and proline; NADH+Succinate+Proline (NSPro) pathways). In chamber B, the specific pathway or complex was measured: the NADH pathway through CI (with pyruvate, glutamate, malate, ADP, and cytochrome *c*), the Succinate pathway through CII (with succinate, rotenone, ADP, and cytochrome *c*), or CIV (pyruvate, malate, glutamate, ADP, cytochrome *c*, succinate, proline, rotenone, antimycin A, ascorbate, and TMPD). Once the O_2 flux stabilized in both chambers, the specific inhibitor of CI (rotenone), CII (malonic acid), or CIV (sodium azide) was titrated. In both chambers determining the control by CI, a titration with rotenone was performed with 13-17 titration points and a final concentration between 0-3.00 µM. In both chambers determining the control by CII, a titration with malonic acid was performed with 12 to 21 titration points and a final concentration between 0-25.5 mM. In both chambers determining the control by

CIV, a titration with sodium azide was performed with 14 titration points and a final concentration between 0-108 mM. Each protocol (chamber A and B for each of the inhibitor) was repeated 5-10 times with male beetles aged 1 and 5 days-old and in both beetle selection lines. Each titration protocol was tested in beetles beforehand to ensure that the appropriate inhibitor concentrations and volumes were titrated to obtain a proper titration curve and to reach complete inhibition.

2.6 Citrate synthase enzyme assays

A portion of each homogenate remaining in the chambers was stored at -80°C for citrate synthase (CS) activity measurement at 30°C, as previously described (Scott et al., 2019; Srere, 1969). Enzymatic activity was expressed in international units (IU) of CS activity per milligram of sample, where IU is one μmol of substrate transformed per minute.

2.7 Data analysis

High-resolution respirometry data analysis was completed using Datlab 7.4 software (OROBOROS Instruments Inc.). Data were adjusted for the instrumental and chemical backgrounds. Mitochondrial respiration was expressed in Flux per mass (pmol O_2 per second per milligram tissue mass corrected for ROX), in flux control ratio (FCR; the pathway or complex in question normalized to maximal OXPHOS capacity of the combined NSPro flux), or per IU of CS activity. The cytochrome *c* effect was calculated using the following equation: [(OXPHOS flux with cytochrome *c* - OXPHOS flux without cytochrome *c*) ÷ OXPHOS flux with cytochrome *c*].

For determining pathway control, mitochondrial respiration was expressed in Flux per mass (pmol O_2 per second per milligram tissue mass) corrected for ROX. Raw data points from each animal homogenate (i.e., chambers A and B) were plotted as threshold plots with relative NSPro flux as a function of relative complex inhibition using Microsoft Excel 2019 (Version 2210). The best-fitting polynomial trendline for each threshold plot was applied based on the accuracy of the curve to the data and the R^2. The order of polynomials varied between 3 and 6. Afterwards, using the specific polynomial curve equation for each animal, the amount of inhibition of the overall flux after 25 and 50% inhibition of the specific complex was determined and then compared between the beetle ages and selection lines. In addition to this analysis, we determined the slope and y-intercept of each animal's CIV threshold plot, using only the data points that indicated CIV inhibition (i.e., after the initial plateau where relative NSPro flux remained unaffected by CIV inhibition).

2.8 Statistical analysis

SigmaPlot 13 (Aspire Software International, Ashburn, VA, USA) was used to complete statistical analyses for all data. In most cases, two-way ANOVAs were used, with the beetle line and age as the two factors. If needed, data were transformed in order to meet the normality and equal variance requirements. Transformations are specified in the description of each figure. The criteria for normality and homogeneity of variance were tested for each variable using Shapiro-Wilk and Brown-Forsythe tests, respectively. If the two requirements were not met, the effects of age and line were considered separately. For the effect of age, we used a one-way ANOVA (followed by a Tukey test) or a Kruskal-Wallis ANOVA on ranks (followed by Dunn's test). For the effect of

the selection line (i.e., longevity), t-tests were completed if both tests passed, and otherwise Mann-Whitney rank sum tests or Kruskal-Wallis ANOVA on ranks were completed. FAO data as well as differences between lines for 25 and 50% inhibition were analyzed using t-tests, with verification of the requirement of normality and equal variance using Shapiro-Wilk and Brown-Forsythe tests, respectively. The y-intercepts and slopes of the CIV titration curves were analyzed using a 2-way ANOVA. Significance was considered at $P \leq 0.05$. Figures were prepared using GraphPad Prism 9.

3. RESULTS

3.1 Body mass

The whole-body weight of each beetle was measured and compared between the selection lines and the ages studied. The body weight showed a decrease with age in both sexes and selection lines (Fig. 2A and B; $P < 0.001$ for both lines in females and in males). In females, this decrease was present between days 1 and 5 only in the E line ($P < 0.001$ for the E line and $P = 0.080$ for the L line), in both lines between days 1 and 8 (Fig. 2A; $P < 0.001$ for both selection lines), and only in the L line between days 5 and 8 (Fig. 2A; $P = 0.006$ for the L line and $P = 0.165$ for the E line). In males, this decrease was present between days 1 and 5 in both selection lines (Fig. 2B; $P < 0.001$ for both), between days 1 and 8 (Fig. 2B; $P < 0.001$ for both selection lines), but only in the L line between days 5 and 8 (Fig. 2B; $P = 0.006$ for the L line and $P = 0.755$ for the E line). The effect of the selection line was evident at days 1 and 5 in both sexes, where L line beetles consistently had a larger mass than E line beetles (Fig. 2A, B; $P < 0.001$ in each case). At day 8, the significance between the lines was lost in both females (Fig. 2A; $P = 0.051$) and males (Fig. 2B; $P = 0.128$).

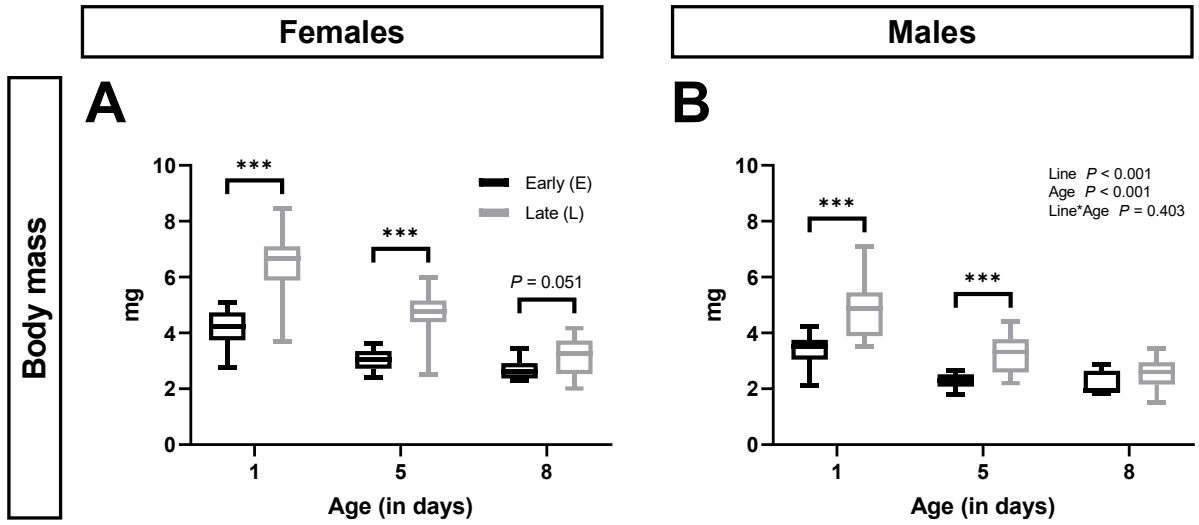

Figure 2: Body mass of female and male beetles of various ages and selection lines. Data for female seed beetles are shown in panel A (n = 14-18 in E line, 15-17 in L line). Data for male seed beetles are shown in panel B (n = 14-16 for days 1 and 5, 4 for day 8 in E line, 13 for days 1, 5, and 8 in L line). Box plots indicate the minimum, 25th percentile, median, 75th percentile, and maximum. Data for males (panel B) met the assumptions of the two-way ANOVA (results presented on the graph), without transformation. Data in panel A did not meet the assumptions and the following tests were performed: one-way ANOVA (age effect within E line) and Kruskal-Wallis ANOVA on ranks (age effect within L line and effect of selection line at each day). Significant differences between the beetle lines for specific ages are denoted *** ($P \leq 0.001$).

3.2 Mitochondrial content

Both CS and CIV activities expressed per mg of tissue are considered biomarkers of mitochondrial content (Boushel et al., 2007; Larsen et al., 2012; Picard et al., 2011). Figure 3 presents the changes in these two biomarkers with age and longevity in the beetle selection lines (E and L lines). The results for CS showed a general increase with age (day) in both females (Fig. 3A; $P < 0.001$) and males (Fig. 3B; $P < 0.001$). The same results were observed for CIV activity in both females (Fig. 3C; $P < 0.001$) and males (Fig. 3D; $P < 0.001$). The two markers of mitochondrial content also showed an effect of the beetle selection line, except for CIV in males which did not reach significance (Fig. 3D; $P = 0.179$). However, CS activity is considered a stronger marker of mitochondrial content (Larsen et al., 2012). In females, both markers showed less mitochondrial content in the L line compared to the E line, which reached significance at days 1 and 5 for CS activity (Fig. 3A; $P = 0.013$ and $P < 0.001$ for days 1 and 5, respectively) and at day 1 for CIV (Fig. 3C; $P < 0.001$). Similarly in males, CS activity showed less mitochondrial content in the L line compared to the E line, which reached significance at days 1 and 5 (Fig. 3B; $P = 0.032$ and $P < 0.001$ for days 1 and 5, respectively). The CS results also showed an interaction between the effect of age and the effect of selection line in both females ($P = 0.010$) and males ($P < 0.001$).

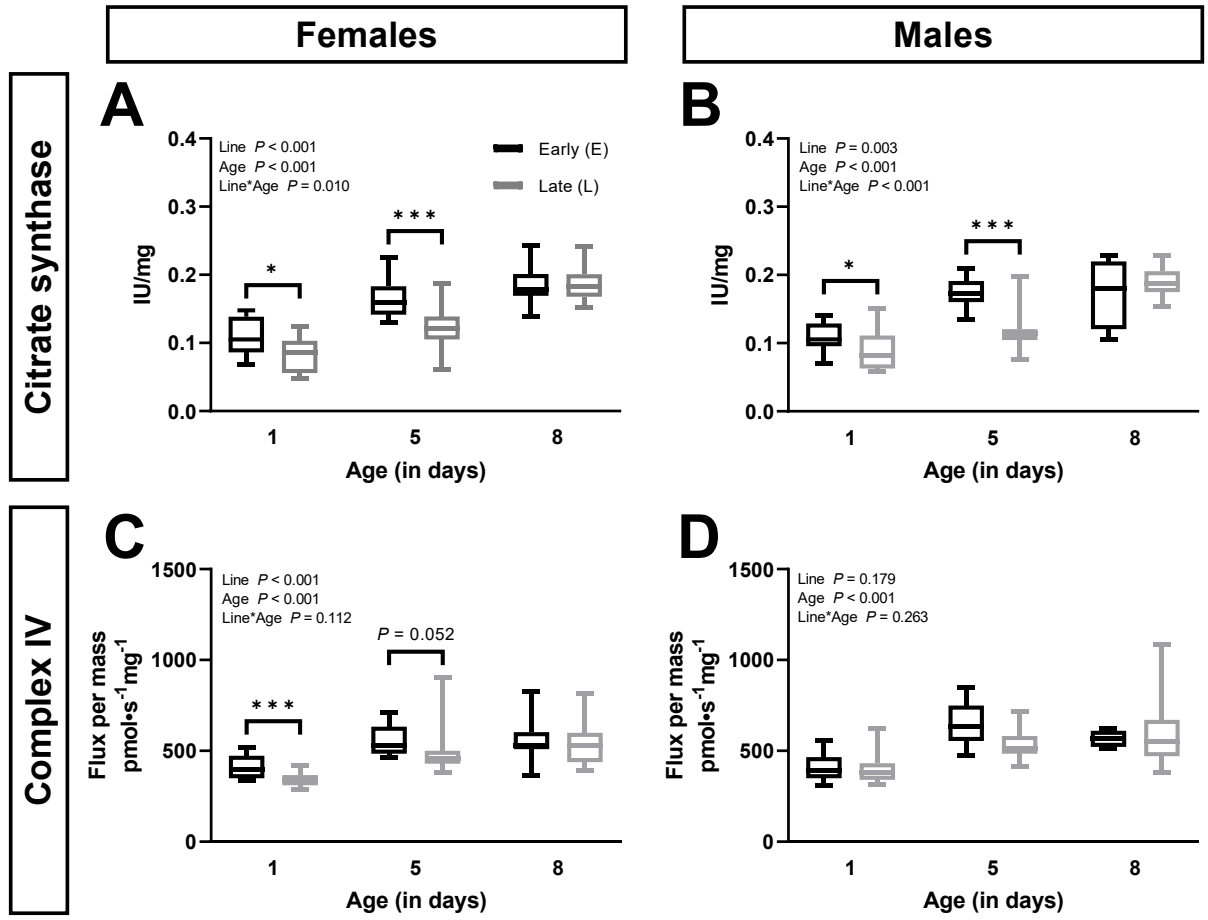

Figure 3: Biomarkers of mitochondrial content in females and males of various ages and selection lines. Citrate synthase (CS) is expressed in specific activity per milligram of seed beetle tissue (panels A, B). Complex IV (CIV) is expressed in Flux per mass of seed beetle tissue (panels C, D). Box plots indicate the minimum, 25th percentile, median, 75th percentile, and maximum. Females n = 14-18 in E line, 15-17 in L line; males n = 14-16 (days 1 and 5) and 4 (day 8) in E line, 13 in L line. Two-way ANOVA P-values for the lines and ages as well as the interaction between lines and ages are indicated in each panel. CS data did not undergo any transformations. CIV data underwent reciprocal (panel C) and natural logarithmic (panel D) transformations to meet the assumptions of the ANOVA. Significant differences between the beetle lines for specific ages are denoted * ($P \leq 0.05$) and *** ($P \leq 0.001$).

3.3 Effect of age and selection line on the NADH pathway through complex I

Interestingly, even if the biomarkers of mitochondrial content showed an increase with age in both sexes, the respiration of the NADH pathway through CI in Flux per mg of tissue showed no change with age, neither in females (Fig. 4A; $P = 0.062$) nor in males (Fig. 4B; $P = 0.056$ in the E line and $P = 0.437$ in the L line). The statistics showed an effect of the selection line on respiration through the NADH pathway in Flux per mass, with more specifically a lower flux in the L line compared to the E line in females (Fig. 4A) at days 1 ($P = 0.023$), 5 ($P = 0.016$) and 8 ($P = 0.026$), and in males (Fig. 4B) at days 1 ($P = 0.010$) and 5 ($P = 0.005$), but not at day 8 ($P = 0.126$).

We investigated further with the FCR values (Fig. 4C, D), which are the Flux per mass normalized to the maximal respiratory capacity with substrates feeding electrons simultaneously into the NADH, Succinate, and Proline pathways. The FCR represents the contribution of a specific pathway to the total OXPHOS capacity (or ET, here equivalent) and therefore the FCR results are dictated by qualitative mitochondrial properties rather than by mitochondrial content. The FCR for the NADH pathway decreases with age in both females (Fig. 4C; $P < 0.001$) and males (Fig. 4D; $P < 0.001$ in the E line and $P = 0.011$ in the L line). In males, the effect of age was more pronounced in younger ages (Fig. 4D; $P < 0.001$ and $P = 0.008$ between days 1 and 5 for E and L lines, respectively; $P = 0.669$ and $P = 0.266$ between day 5 and 8 for E and L lines, respectively), whereas in females, the effect of age was less pronounced and reached significance only between days 1 and 8 (Fig. 4C; $P < 0.001$ for the E line and $P = 0.001$ for the L line) and between days 5 and 8 in the L line (Fig. 4C; $P = 0.042$). The L line showed a lower NADH pathway flux through CI compared to the E line. In females (Fig. 4C), the effect of selection line was significant at days 1 ($P = 0.011$) and 8 ($P = 0.024$), whereas in males (Fig. 4D), it was significant at days 1 ($P =$

0.004) and 5 (P = 0.002).

When the data were expressed in Flux per IU CS (Fig. 4E, F), the same pattern of a decrease with age was observed as when in FCR, both in females (Fig. 4E; $P < 0.001$) and in males (Fig. 4F; $P < 0.001$). There was a continual decrease throughout the study period in females (Fig. 4E; P = 0.002 between days 1 and 5 and P = 0.010 between days 5 and 8), whereas in males, the differences were only observed between days 1 and 5 (Fig. 4F; P = 0.001) and not between days 5 and 8 (Fig. 4F; P = 0.494). Because of the increase in variability resulting from incorporating the CS IU in the results, the differences between the lines were lost (Fig. 4E, F; P = 0.820 in females and P = 0.273 in males).

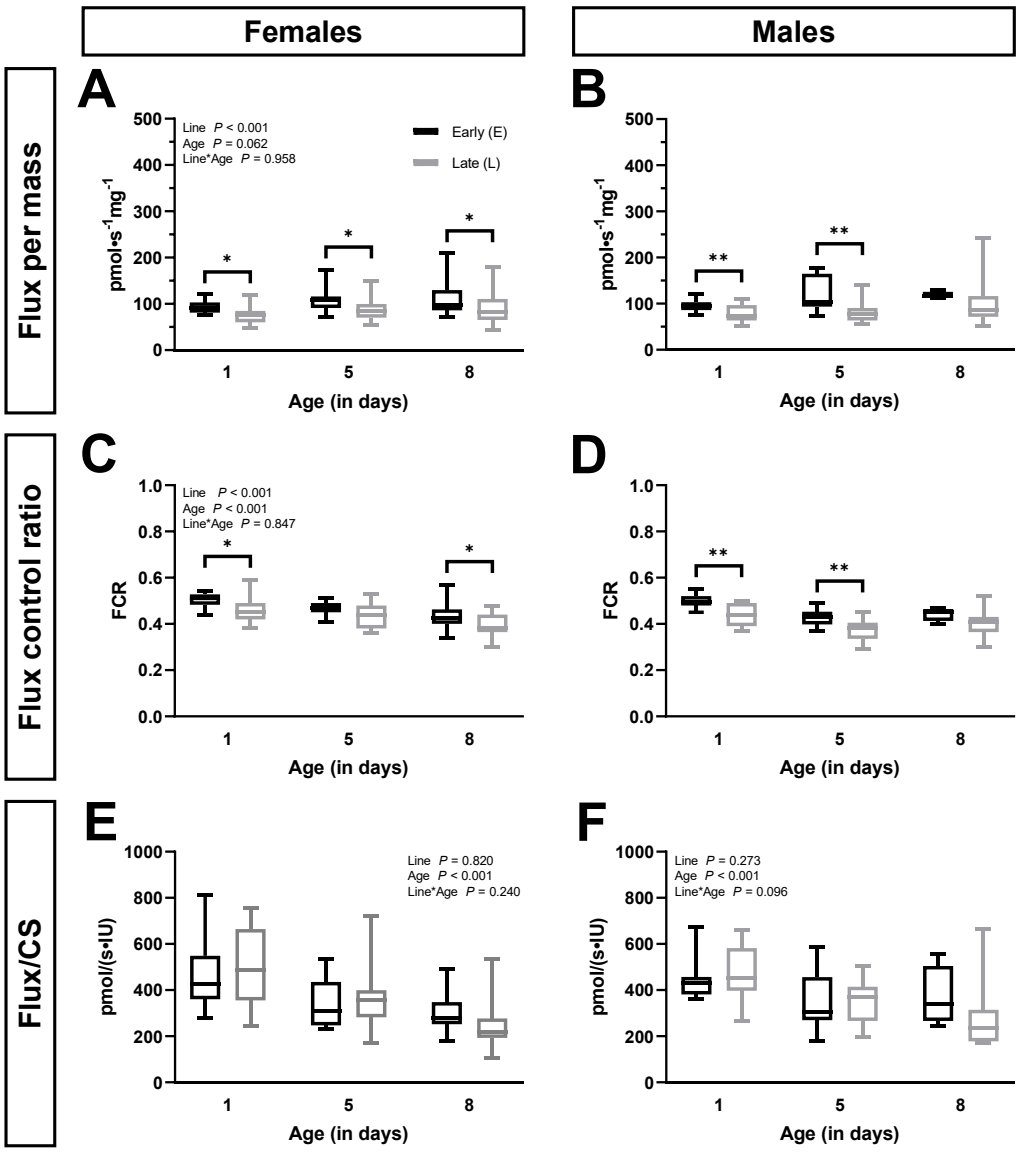

Figure 4: NADH pathway capacity in females and males of various ages and selection lines. Results for the NADH pathway through complex I are presented in Flux per mass (pmol·s^{-1}mg^{-1}; panels A and B), FCR (panels C and D), and Flux per international unit (IU) of CS (pmol/(s·IU); panels E and F) in seed beetle tissue at days 1, 5, and 8 of their lifespan. Data for female seed beetles is shown in panels A, C, and E (n = 14-18 in the E line, 15-17 in the L line). Data for male seed beetles is shown in panels B, D, and F (n = 14-16 for days 1 and 5, 4 for day 8 in the E line, 13 for all timepoints in the L line). Box plots indicate the minimum, 25th percentile, median, 75th percentile, and maximum. Two-way ANOVA P-values for the lines and ages as well as the interaction between line and age are indicated in panels whose data met the assumptions of the ANOVA, with the following transformations: base 10 logarithm in A, no transformation in C, square root in E, and natural logarithm in F. Data in panels B and D did not meet the assumptions and the following tests were performed: one-way ANOVA (age effect within each line in panel D), Kruskal-Wallis ANOVA on ranks (age effect within each line in panel B), t-test (selection line effect at day 1 in panel B and line effect at days 5 and 8 in panel D), and Mann-Whitney sum test (selection line effect at days 5 and 8 in panel B, and selection line effect at day 1 in panel D). Significant differences between the beetle lines are denoted * ($P \leq 0.05$) and ** ($P \leq 0.01$).

3.4 Effect of age and selection line on the Succinate pathway through complex II

The Succinate pathway through CII generally showed a very distinct effect compared to the NADH pathway through CI. When expressed in Flux per mass, the Succinate pathway followed a similar increase with age as observed for the markers of mitochondrial content in both females (Fig. 5A; $P < 0.001$ for both E and L lines) and males (Fig. 5B; $P < 0.001$). Females of both lines had significant increases between days 1 and 5 (Fig. 5A; $P = 0.003$) and days 1 and 8 (Fig. 5A; $P < 0.001$). Similarly, males showed increases between days 1 and 5 and days 1 and 8 (Fig. 5B; $P < 0.001$ for both), but not between days 5 and 8 (Fig. 5B; $P = 0.995$). The use of rotenone in the presence of proline inhibits CI but only part of the ProDH pathway (Teulier et al., 2016). So here, the Succinate pathway was measured in some presence of the ProDH pathway. As a result, the increase in the Flux per mass of the Succinate pathway with age could be overestimated because the ProDH pathway also had an increase in Flux per mass with age (see below). The Succinate pathway in Flux per mass did not show any significant differences linked to selection lines both in females (Fig. 5A; $P = 0.067$ at day 1, $P = 0.070$ at day 5, $P = 0.704$ at day 8) and in males (Fig. 5B; $P = 0.283$).

When expressed in FCR, both females (Fig. 5C) and males (Fig. 5D) showed a significant effect of age ($P < 0.001$ in both females and males) and line ($P = 0.032$ in females and $P = 0.003$ in males), but no interaction between the two factors ($P = 0.854$ in females and $P = 0.202$ in males). Contrary to the NADH pathway, the Succinate pathway's contribution through CII (i.e., the FCR) increased with age in both sexes (Fig. 5C and 5D; $P < 0.001$ for both). In females, significant increases were obtained between days 1 and 5 (Fig. 5C; $P = 0.008$) and between days 1 and 8 (Fig. 5C; $P < 0.001$). In males, the same was observed (Fig. 5D; $P < 0.001$ and $P = 0.004$ for between

days 1 and 5 and days 1 and 8, respectively). Since the Succinate pathway's FCR saw an increase with age even though the ProDH pathway decreased with age (see below), the Succinate pathway's FCR may actually be higher than what is shown in the figures. Regarding the effect of the selection line, the L line showed a stronger contribution of the Succinate pathway to OXPHOS compared to the E line. This effect is contrary to what was observed in the NADH pathway. The effect of the selection line on the Succinate pathway was also less pronounced in females (Fig. 5C; $P = 0.032$ and not significant at specific time points) compared to males (Fig. 5D; $P = 0.003$ and significant at 1 and 5 days, but not at 8 days).

Normalized to CS, both females (Fig. 5E) and males (Fig. 5F) showed a significant effect of age ($P < 0.001$ in females and $P = 0.030$ in males) and selection line ($P = 0.027$ in females and $P = 0.026$ in males). But in contrast to the data in FCR, there was also a significant interaction between the two factors in both females ($P = 0.040$) and males ($P = 0.006$). In females, there was a decrease in Flux/CS with age in the L line between days 1 and 8 (Fig. 5E; $P < 0.001$) and between days 5 and 8 (Fig. 5E; $P = 0.009$). In the E line, no significant differences were noted. The same pattern occurred in males where only the L line presented a significant decrease in the Succinate pathway Flux/CS with age (Fig. 5F; $P < 0.001$ for between both ages 1 and 8 and ages 5 and 8), and not the E line. A significantly higher Succinate pathway capacity normalized to CS activity occurred in L line females at days 1 and 5 (Fig. 5E; $P = 0.024$ and $P = 0.027$ for days 1 and 5, respectively) and in L line males at days 1 (Fig. 5F; $P = 0.002$) and 5 (Fig. 5F; $P < 0.001$) compared to the E line.

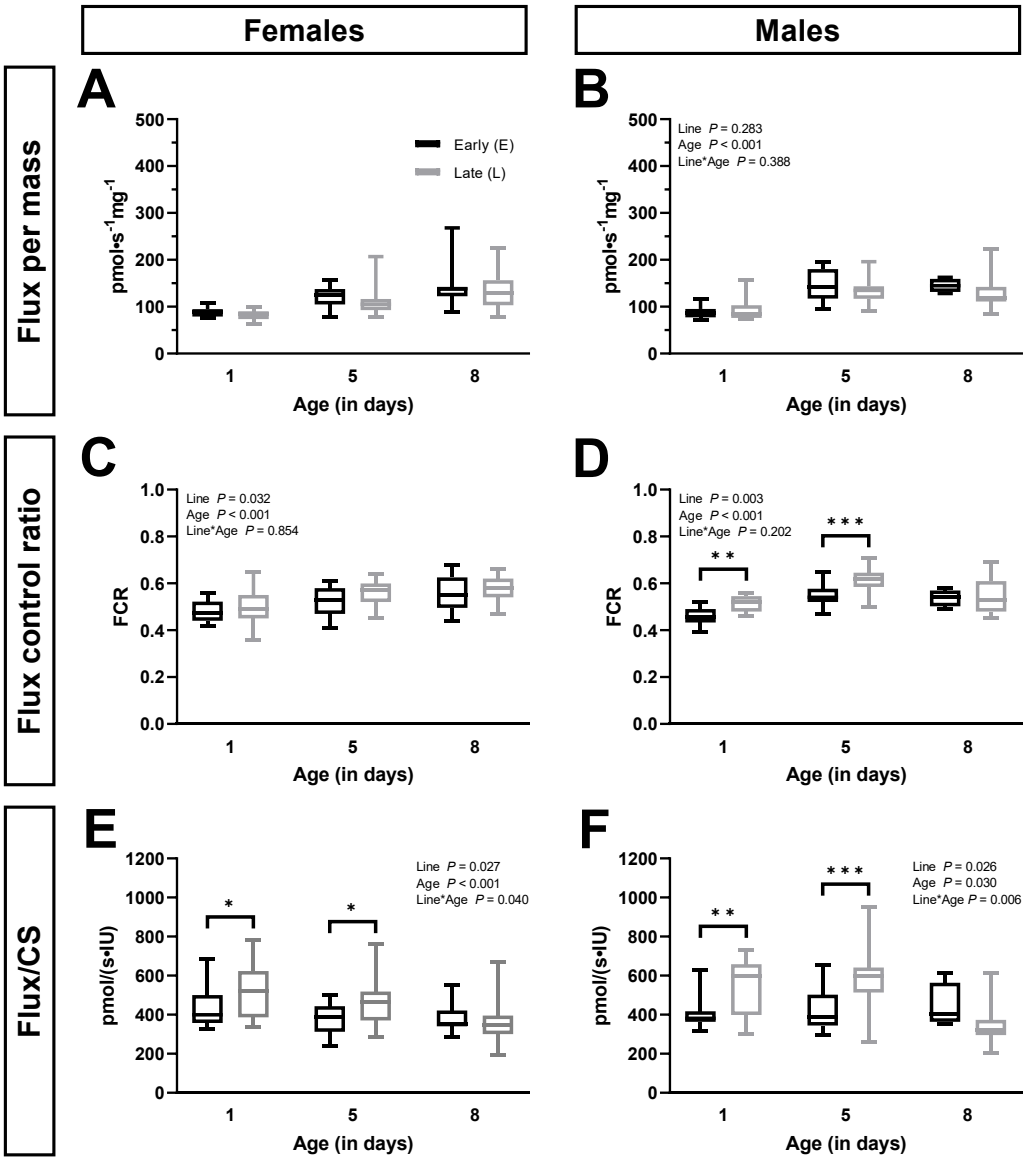

Figure 5: Succinate pathway capacity in females and males of various ages and selection lines. Results for the Succinate pathway through complex II are presented in Flux per mass (pmol·s^{-1}mg^{-1}; panels A and B), FCR (panels C and D), and Flux per international units (IU) of CS (pmol/(s· IU); panels E and F) in seed beetle tissue at days 1, 5, and 8 of their lifespan. Data for female seed beetles are shown in panels A, C, and E (n = 14-18 in the E line, 15-17 in the L line). Data for male seed beetles are shown in panels B, D, and F (n = 14-16 for days 1 and 5, 4 for day 8 in the E line, 13 for all timepoints in the L line). Box plots indicate the minimum, 25th percentile, median, 75th percentile, and maximum. Two-way ANOVA P-values for the lines and ages as well as the interaction between line and age are indicated in panels whose data met the assumptions of the ANOVA, with the following transformations: reciprocal transformation in B, no transformation in C, D, and F, and square root transformation in E. Data in panel A did not meet the assumptions and the following tests were performed: one-way ANOVA (age effect in the L line with natural logarithm transformation), Kruskal-Wallis ANOVA on ranks (age effect in the E line), t-test (selection line effect at day 1) and Mann-Whitney rank sum test (selection line effect at days 5 and 8). Significant differences between the beetle lines are denoted * ($P \leq 0.05$), ** ($P \leq 0.01$), and *** ($P \leq 0.001$).

3.5 Ratio of the NADH or the Succinate pathway over complex IV activity

The ratios of the NADH pathway over CIV and the Succinate pathway over CIV (Fig. 6) showed the same general results as the FCR or Flux/CS, i.e., there was (1) a decrease in the NADH pathway capacity and an increase in the Succinate pathway with age, and (2) a lower NADH pathway capacity in the L line compared to the E line.

The NADH pathway decreases with age in both females and males (Fig. 6A and B; $P < 0.001$ for both sexes). Females specifically saw decreases between days 1 and 8 ($P < 0.001$) and between days 1 and 5 ($P = 0.001$). Likewise in males, the effect of age was also observed between days 1 and 8 ($P = 0.035$) and between days 1 and 5 ($P < 0.001$). The NADH pathway over CIV had an overall effect of the beetle selection lines, with the L line having a lower ratio than the E line ($P = 0.014$ in females, $P < 0.001$ in males). Only at day 8 was there a significant difference between the lines in females ($P = 0.023$), but males had significant differences at all time points studied ($P = 0.004$ for day 1, $P = 0.030$ for day 5, and $P = 0.035$ for day 8).

The Succinate pathway over CIV only showed a significant increase with age in females (Fig. 6C; $P = 0.003$), but showed a trend of an increase with age in males (Fig. 6D; 0.062). In females, there was a significant increase between days 1 and 8 ($P = 0.038$) and between days 5 and 8 ($P = 0.004$). There was no effect of beetle selection line in females nor males ($P = 0.346$ and $P = 0.853$, respectively), but there was an interaction between selection line and age in males (Fig. 6D; $P = 0.013$).

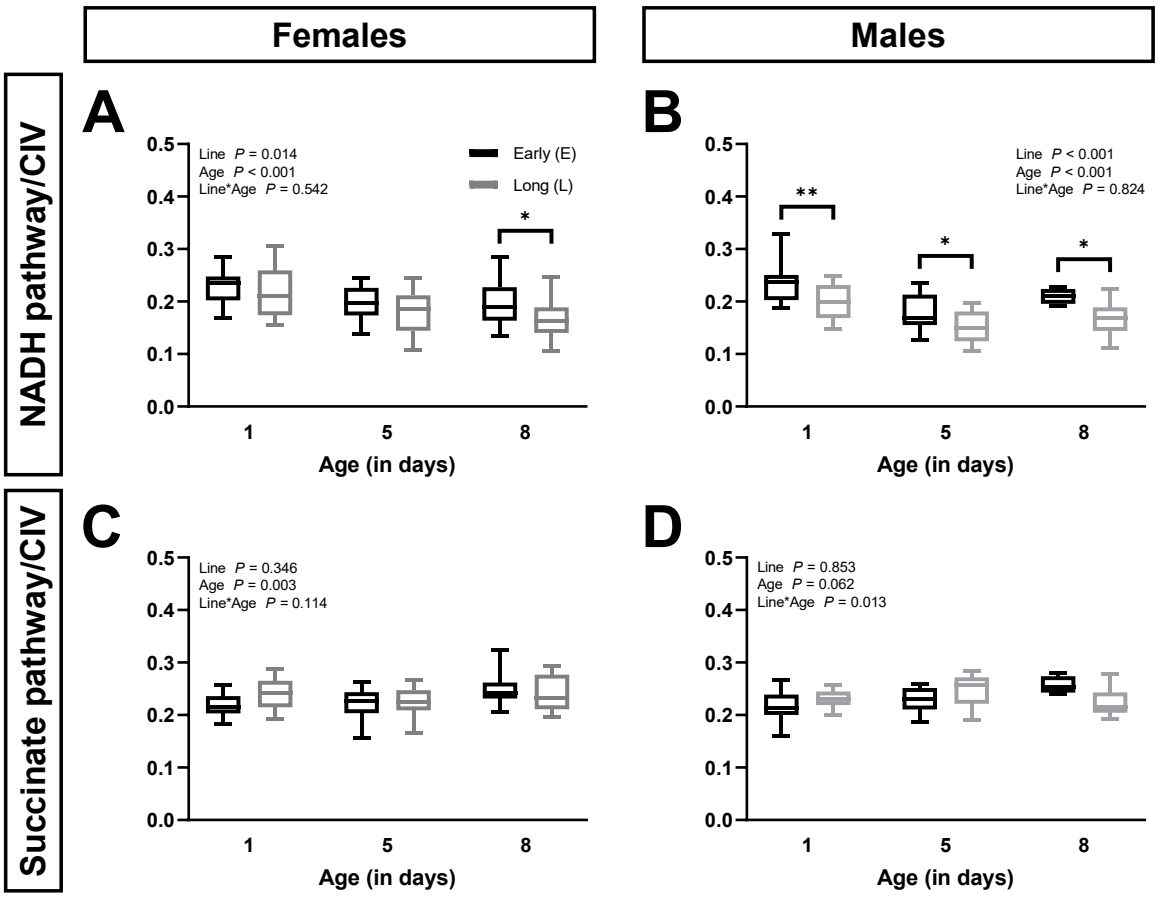

Figure 6: Ratio of the NADH and the Succinate pathway over complex IV activity in females and males of various ages and selection lines. Ratios for the NADH pathway capacity (panels A and B) and for the Succinate pathway capacity (panels C and D) are presented for seed beetles at days 1, 5, and 8 of their lifespan. Data for female beetles are shown in panels A and C (n = 14-18 in the E line, 15-17 in the L line). Data for male beetles are shown in panels B and D (n = 14-16 for days 1 and 5, 4 for day 8 in the E line, 13 for all timepoints in the L line). Box plots indicate the minimum, 25th percentile, median, 75th percentile, and maximum. Two-way ANOVA P-values for the lines and ages as well as the interaction between line and age are indicated. Data in panels A, B, C, and D did not undergo any transformations. Significant differences between the beetle lines are denoted * ($P \leq 0.05$) and ** ($P \leq 0.01$).

3.6 Effect of age and selection line on the Proline dehydrogenase (ProDH) pathway

In order to calculate the contribution of the ProDH pathway flux to maximal respiration (Fig. 7A, B), we subtracted the combined NS pathway flux from the maximum flux with the NADH, Succinate, and Proline pathways active. Only an effect of age was noted when the data were expressed in Flux per mass (Fig. 7A, B; $P = 0.027$ in females and $P = 0.009$ in males), in FCR (Fig. 7C and D; $P = 0.019$ in females and $P = 0.003$ in males), and in Flux/CS IU (Fig. 7E, F, $P < 0.001$ in both females and males). In Flux per mass, the flux through the ProDH pathway increased with age in both sexes, and significance was attained between days 1 and 8 (Fig. 7A, B; $P = 0.022$ and $P = 0.008$, in females and males, respectively). When the data were expressed in FCR (Fig. 7C, D) or in Flux per CS (Fig. 7E, F), the effect was a decrease with age. Significant differences were obtained in FCR between days 1 and 8 in females (Fig. 7C; $P = 0.017$) and between days 1 and 5 in males (Fig. 7D; $P = 0.002$). In Flux per CS, there was a decrease between days 1 and 5 (Fig. 7E, F; $P = 0.002$ in both males and females) and between days 1 and 8 ($P = 0.002$ in males and $P < 0.001$ in females). No effect of the selection line occurred in any of the units (Fig. 7A-F).

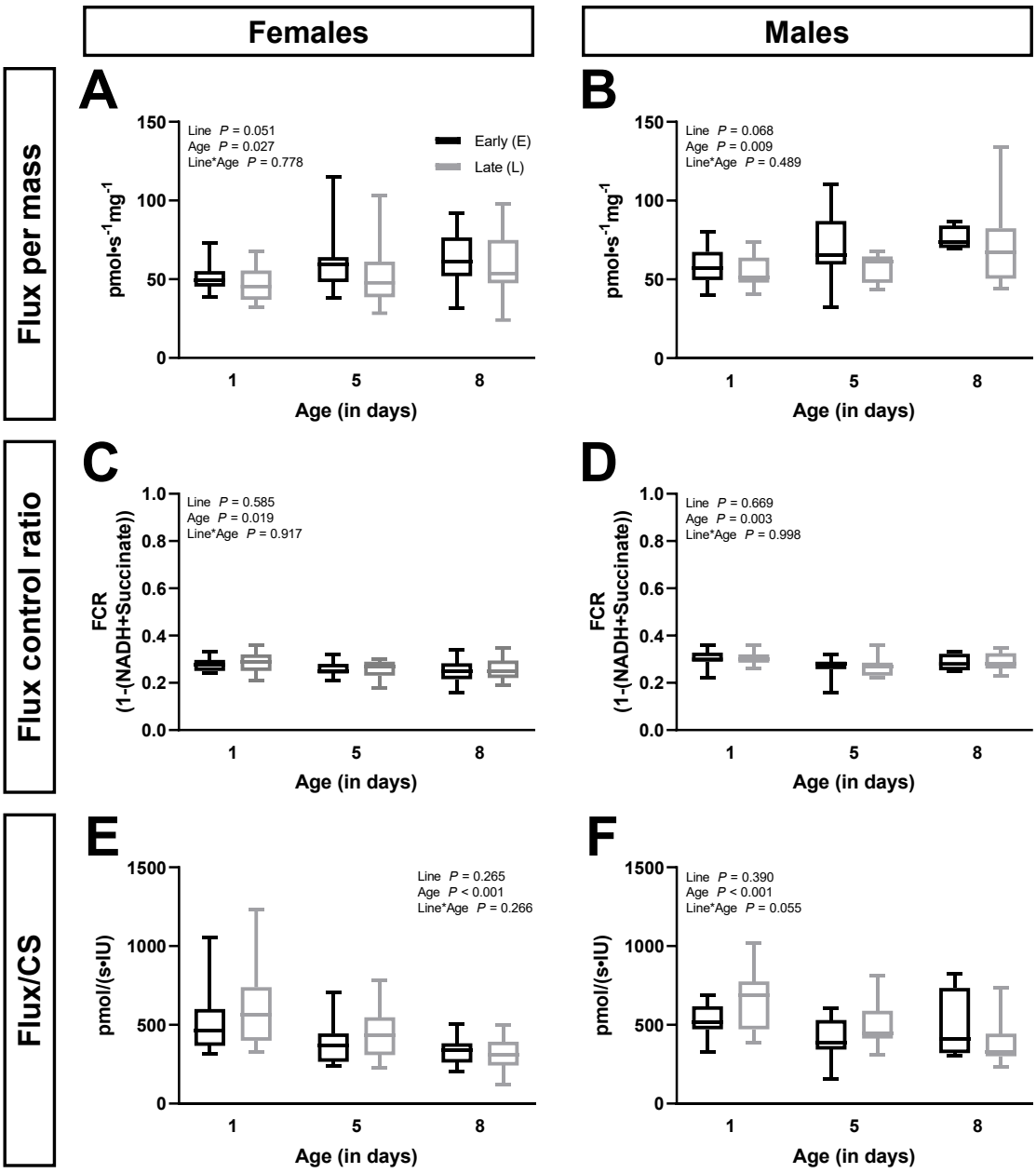

Figure 7: Proline dehydrogenase pathway capacity in females and males of various ages and selection lines. Results for the Proline dehydrogenase pathway are presented in Flux per mass (pmol·s^{-1}mg^{-1}; panels A and B), FCR (panels C and D), and Flux per international units (IU) of CS (pmol/(s·IU); panels E and F) in seed beetle tissue at days 1, 5, and 8 of their lifespan. Data for female seed beetles are shown in panels A, C, and E (n = 14-18 in the E line, 15-17 in the L line). Data for male seed beetles are shown in panels B, D, and F (n = 14-16 for days 1 and 5, 4 for day 8 in the E line, 13 for all timepoints in the L line). Box plots indicate the minimum, 25th percentile, median, 75th percentile, and maximum. Two-way ANOVA P-values for the lines and ages as well as the interaction between line and age are indicated in panels whose data met the assumptions of the ANOVA. Data in panels A, B, E, and F underwent square root transformations to meet the assumptions of the ANOVA. Data in panels C and D did not undergo any transformations.

3.7 Effect of age and selection line on the NADH+Succinate+Proline (NSPro) combined pathway flux

The combined NSPro flux was the maximal, combined pathway flux measured in this study. When expressed in Flux per mass, the combined NSPro flux showed an increase with age in both females and males (Fig. 8A, B; $P < 0.001$ for both). Significant differences for Flux per mass were obtained between days 1 and 5 (Fig. 8A; $P = 0.001$) and between days 1 and 8 (Fig. 8A; $P < 0.001$) in females. In males, the same differences were present (Fig. 8B; $P < 0.001$ between days 1 and 5 and between days 1 and 8). There was also an effect of the beetle selection line on the combined NSPro flux in Flux per mass, with the L line presenting a lower flux than the E line in females (Fig. 8A; $P < 0.001$) and males (Fig. 8B; $P = 0.006$). In females, the selection line effect was statistically significant at days 1 (Fig. 8A; $P = 0.044$) and 5 (Fig. 8A; $P = 0.032$). In males, significance was reached at day 5 only (Fig. 8B; $P = 0.015$).

When the data were normalized to CS (Fig. 8C, D), the opposite was observed. With age, NSPro Flux/CS decreased in both females (Fig. 8C; $P < 0.001$) and males (Fig. 8D; $P = 0.003$). In females, significant differences were observed between all timepoints studied (Fig. 8C; $P = 0.005$ between days 1 and 5, $P < 0.001$ between days 1 and 8, $P = 0.028$ between days 5 and 8). In males, there was only a significant decrease between days 1 and 8 (Fig. 8D; $P = 0.003$). There were no differences between the lines in females (Fig. 8C; $P = 0.337$) nor in males (Fig. 8D; $P = 0.404$). However, there was an interaction between selection line and age in males only (Fig. 8D; $P = 0.027$).

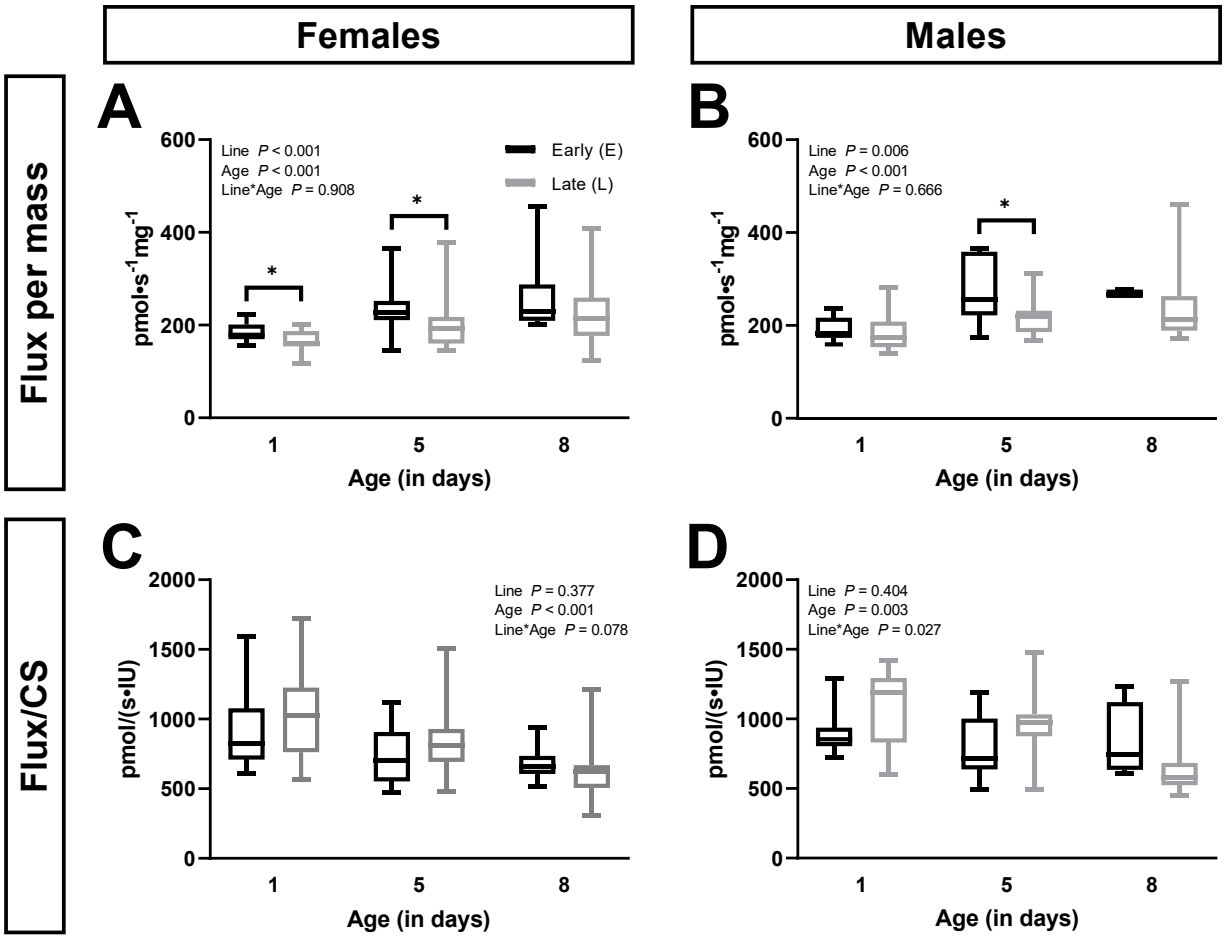

Figure 8: The combined NADH+Succinate+Proline (NSPro) pathway capacity in females and males of various ages and selection lines. Results for the NSPro pathway are presented in Flux per mass (pmol·s^{-1}mg^{-1}; panels A and B) and Flux per international units (IU) of CS (pmol/(s·IU); panels C and D) in seed beetle tissue at days 1, 5, and 8 of their lifespan. Data for female seed beetles are shown in panels A and C (n = 14-18 in the E line, 15-17 in the L line). Data for male seed beetles are shown in panels B and D (n = 14-16 for days 1 and 5, 4 for day 8 in the E line, 13 for all timepoints in the L line). Box plots indicate the minimum, 25th percentile, median, 75th percentile, and maximum. Two-way ANOVA P-values for the lines and ages as well as the interaction between line and age are indicated in panels whose data met the assumptions of the ANOVA. Data in panels A and B underwent reciprocal transformations, data in panel C underwent a natural logarithmic transformation, and data in panel D underwent a square root transformation to meet the assumptions of the ANOVA. Significant differences between the beetle lines are denoted * ($P \leq 0.05$).

3.8 Effect of age and selection line on complex IV activity expressed in FCR and per unit of CS activity

When expressed in FCR (Fig. 9A, B) or in Flux per CS IU (Fig. 9C, D), CIV activity showed an effect of age in females ($P = 0.002$ in FCR and $P < 0.001$ in Flux per CS IU) and males ($P < 0.001$ in FCR and $P = 0.007$ in Flux per CS IU), but the effect of selection lines was only present in males ($P = 0.024$ in FCR and $P = 0.025$ in Flux per CS), with the L line exhibiting higher FCR and Flux per CS IU than the E line. No interaction between the two factors was detected in any sex or unit. With age, the FCR for CIV increased significantly between days 1 and 5 in females (Fig. 9A; $P = 0.002$, both lines confounded), and in males (Fig. 9B; $P < 0.001$, both lines confounded). In females, CIV activity normalized to CS was lower at day 8 compared to days 1 and 5 (Fig. 9C; $P < 0.001$ between days 1 and 8, and 5 and 8). In males, the decrease with age was significant between days 1 and 8 (Fig. 9D; $P = 0.008$) and between days 5 and 8 ($P = 0.013$).

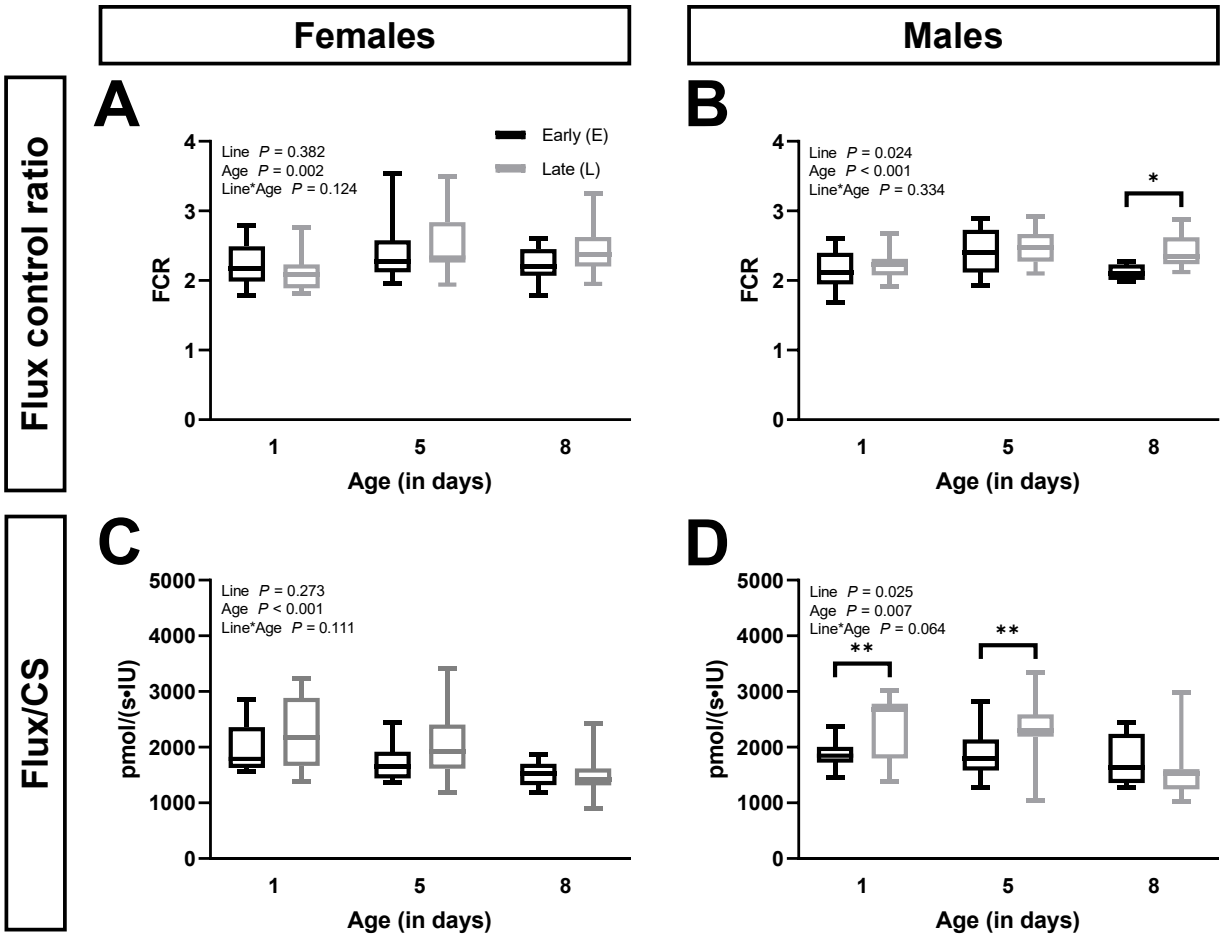

Figure 9: Complex IV activity in females and males of various ages and selection lines. Results for complex IV activity are presented in FCR (panels A and B) and in Flux per international units (IU) of CS (pmol/(s· IU); panels C and D) in seed beetle tissue at days 1, 5, and 8 of their lifespan. Data for female seed beetles are shown in panels A and C (n = 14-18 in the E line, 15-17 in the L line). Data for male seed beetles are shown in panels B and D (n = 14-16 for days 1 and 5, 4 for day 8 in the E line, 13 for all timepoints in the L line). Box plots indicate the minimum, 25th percentile, median, 75th percentile, and maximum. Two-way ANOVA P-values for the lines and ages as well as the interaction between line and age are indicated in each panel. Data in panels A and C underwent reciprocal transformations to meet the assumptions of the ANOVA. Data in panels B and D did not undergo any transformations. Significant differences between the beetle lines are denoted * ($P \leq 0.05$) and ** ($P \leq 0.01$).

3.9 Effect of selection line on the capacity to oxidize fatty acids

Figure 10 presents the Flux per mass of select fatty acids providing electrons to the Q-junction through the ETF: the long-chain fatty acid palmitoylcarnitine and the medium-chain fatty acid octanoylcarnitine, both in the presence of malate, ADP, and cytochrome *c*. Comparing each beetle selection line, there were no significant differences in FAO for either fatty acid (Fig. 10A, B; $P = 0.180$ and $P = 0.440$, respectively).

Of important note, the capacity to oxidize fatty acids showed up as extremely low, with all fatty acid substrates. With palmitoylcarnitine as the substrate, the capacity expressed in percent as median (min-max) was 13 (9-19)% of the capacity of the NADH pathway. With octanoylcarnitine as the substrate, the capacity was 10 (8-16)% of the capacity of the NADH pathway. We additionally tested the short-chain fatty acid, acetylcarnitine, only in the L line, but again, there was no significant utilization of this fatty acid, and the proportion of its flux compared to the NADH pathway was 10 (10-12)%.

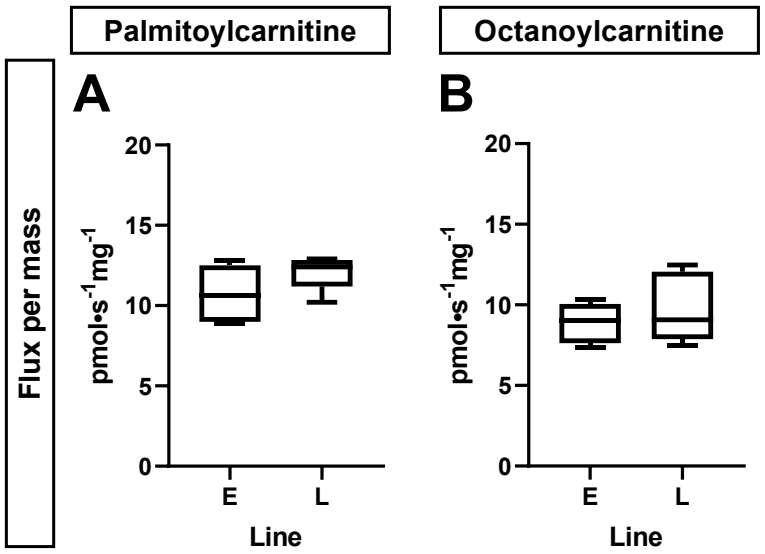

Figure 10: Fatty acid oxidation in males of the two selection lines at day 1. Results for fatty acid oxidation are presented in Flux per mass (pmol·s^{-1}mg^{-1}; panels A and B), not corrected for instrumental background, with palmitoylcarnitine and malate as the substrates in panels A and octanoylcarnitine and malate as the substrates in panel B. n = 5 per box. Box plots indicate the minimum, 25th percentile, median, 75th percentile, and maximum. T-tests were performed and showed no significant differences between the beetle lines.

3.10 Control of the mitochondrial respiratory capacity by complex I, complex II and complex IV

To evaluate the control of one complex on the overall mitochondrial respiratory capacity, we administered an inhibitor titration protocol specific for each complex, i.e., rotenone to inhibit CI within the NADH pathway (Fig. 11), malonate to inhibit CII within the Succinate pathway (Fig. 12), or sodium azide to inhibit CIV (Fig. 13). Only males were studied. For each animal, the inhibitor titration was performed simultaneously on the maximal pathway flux with NSPro activated (oxygraph chamber A) and on the specific complex in question (oxygraph chamber B). This allowed us to both determine any possible excess (i.e., unused) capacity of that complex and also the resulting control of that complex over the overall pathway flux.

The impact of the rotenone titration on the relative NADH pathway (x axis) and on the relative maximal pathway flux (y axis) was displayed as scatter plots (Fig. 11A-D). At day 1 of age, the curve showed a stronger inhibition of the relative NSPro pathway at low relative CI inhibition in the L line (Fig. 11C) compared to the E line (Fig. 11A). In order to measure this effect and detect any possible significance, the amount of inhibition of the overall flux when inhibiting 25 (Fig. 11E) and 50% (Fig. 11F) of CI was compared between beetle selection lines. The calculation was made from the titration curve obtained for each animal. When CI was inhibited in beetles at day 1 of age, the decrease in NSPro pathway flux was stronger in the L line compared to the E line (Fig. 11E; $P = 0.038$ at 25% inhibition, Fig. 11F; $P = 0.028$ at 50% inhibition). At 50% inhibition of CI, E line beetles were still at 69% of maximal NSPro flux (66-84%, min-max), whereas L line beetles were only at 64% of maximal NSPro flux (58-67%, min-max). Since L line beetles already had an initial lower relative CI capacity to begin with (presented in Fig. 4C, D), there was a stronger impact of rotenone inhibition compared to in E line beetles. In other words, there is little to no excess CI capacity in L line beetles, so CI inhibition more strongly controls overall pathway flux. Furthermore, the control by CI did not change as E line beetles aged (Fig. 11E, F; $P = 0.804$ at 25% inhibition; $P = 0.551$ at 50% inhibition), but tended to decrease (i.e., the overall NSPro flux was less affected, so higher) in the L line with age (Fig. 11E, F; $P = 0.057$ at 25% inhibition; $P = 0.030$ at 50% inhibition). Then, at day 5, the impact of CI inhibition was considered equivalent in both lines, at both 25 (Fig. 11E; $P = 0.627$, 87% and 87% for E and L lines, respectively) and 50% inhibition (Fig. 11F; $P = 0.073$, 75 and 68% in E and L lines, respectively).

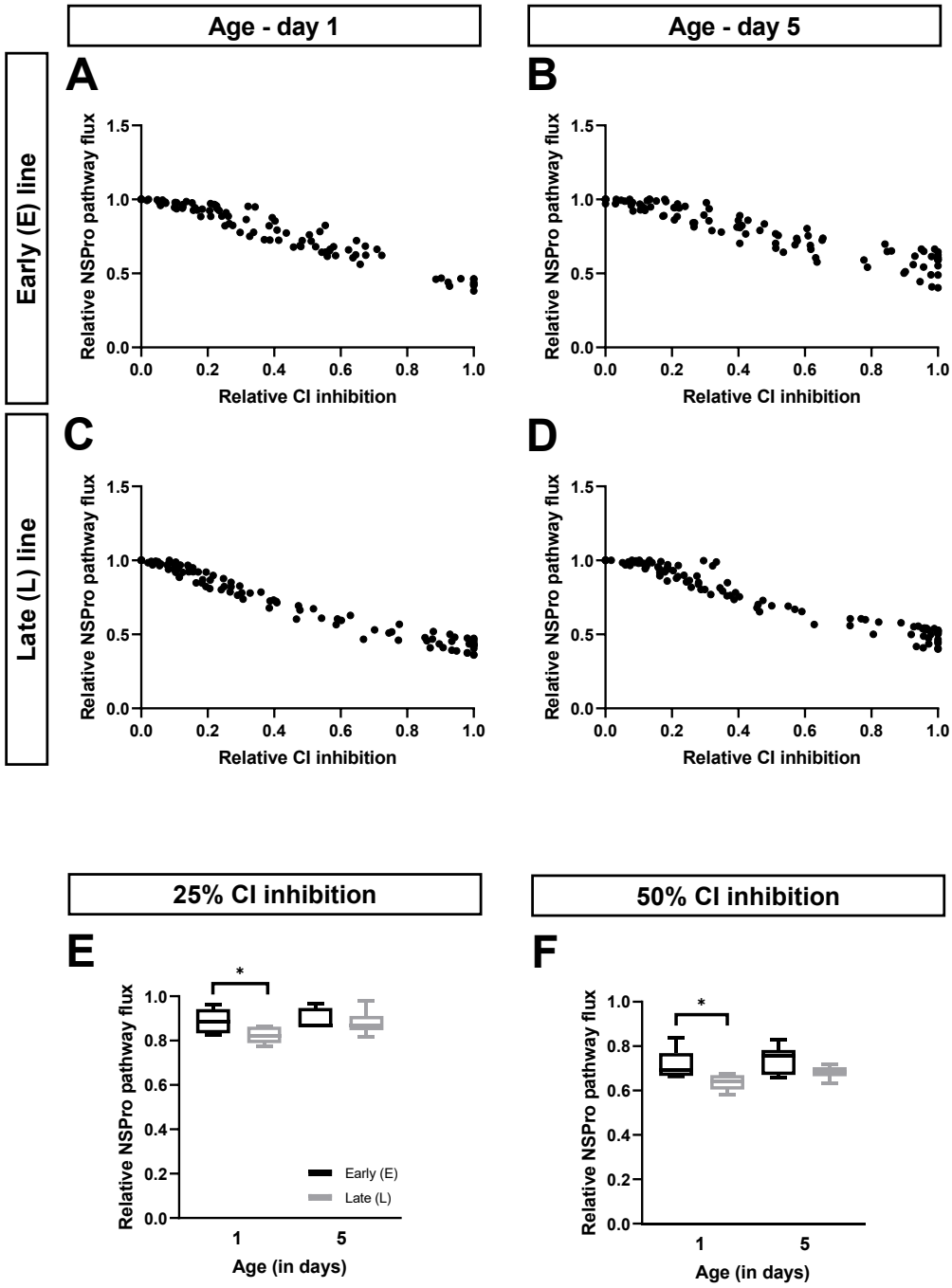

Figure 11: Effect of complex I inhibition on maximal pathway flux. (A-D) The relative maximal pathway flux in the presence of NADH, succinate and proline (NSPro) is presented as a function of relative complex I (CI) inhibition using a rotenone titration at days 1 (panels A and C) and 5 (panels B and D) in males of the early (E; panels A and B) and late (L; panels C and D) seed beetle selection lines. Dots represent the raw data plots. (E-F) The relative NSPro flux at 25% (panel E) and 50% (panel F) CI inhibition, at days 1 and 5 in males of the E and L lines. $n = 6$ at both ages and for both lines. Significant differences between the lines as the result of t-test statistical analyses are denoted * ($P \leq 0.05$).

The impact of the malonate titration on the relative Succinate pathway (x axis) and on the relative maximal pathway flux (y axis) was displayed as scatter plots (Fig. 12A-D). The curve showed a similar repartition of the relative NSPro pathway with CII inhibition in the L compared to the E line at both days 1 and 5. When 25 or 50% of CII was inhibited (Fig. 12E, F), the decrease in NSPro pathway flux was the same in both lines (Fig. 12E, at 25% inhibition, $P = 0.494$ at day 1 and $P = 0.452$ at day 5; Fig. 12F, at 50% inhibition, $P = 0.597$ at day 1 and $P = 0.522$ at day 5). Furthermore, the control by CII did not change with age in the E line (Fig. 12E, F; $P = 0.362$ at 25% inhibition; $P = 0.953$ at 50% inhibition) nor in the L line (Fig. 12E, F; $P = 0.878$ at 25% inhibition; $P = 0.676$ at 50% inhibition). Even if the Succinate pathway compensated for the lack in the NADH pathway in the L line compared to the E line (Fig. 5C, D), CII did not show a change in control over the maximal pathway flux between the lines.

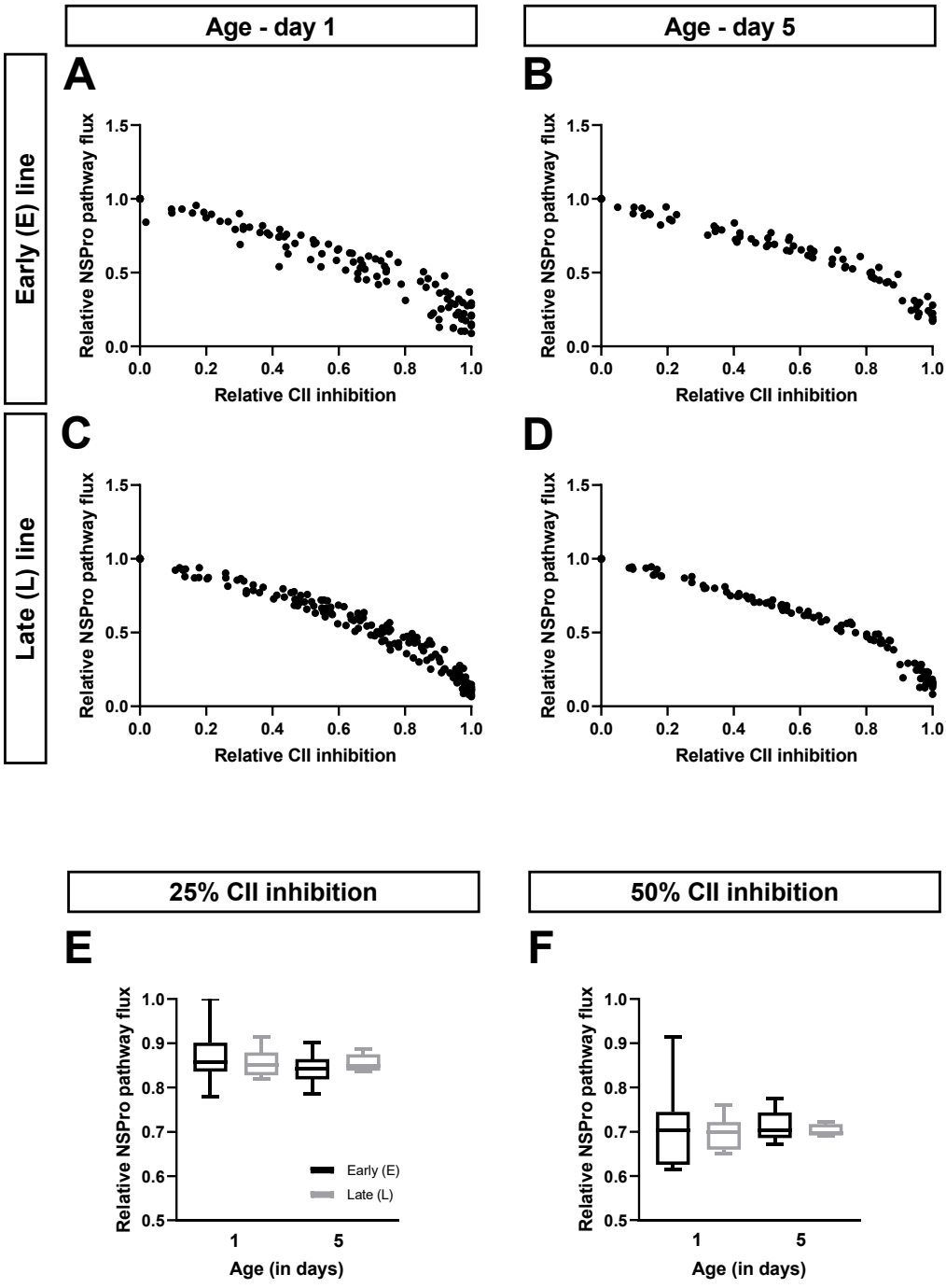

Figure 12: Effect of complex II inhibition on maximal pathway flux. (A-D) The relative maximal pathway flux in the presence of NADH, succinate and proline (NSPro) is presented as a function of relative complex II (CII) inhibition using a malonate titration at days 1 (panels A and C) and 5 (panels B and D) in males of the early (E; panels A and B) and late (L; panels C and D) seed beetle selection lines. Dots represent the raw data plots. (E-F) The relative NSPro flux at 25% (panel E) and 50% (panel F) CII inhibition, at days 1 and 5 in males of the E and L lines. n = 6-7 for the E line and n = 7-10 for the L line at both ages. T-tests were performed and showed no significant differences between the beetle lines.

The apparent excess capacity of downstream complexes (i.e., CIII and CIV) lowers and their flux control increases to support increased electron entry when multiple electron entry pathways into the OXPHOS process are active (here, NADH, Succinate, and ProDH; Lemieux et al., 2017). We therefore examined the apparent excess capacity of CIV at maximal convergent pathway flux through the ETS. These plots (Fig. 13A-D) show two distinct phases: (1) the elimination of excess capacity above the threshold (initial slope; grey dots) and (2) the slope below the threshold (black dots and solid line), where further inhibition of CIV caused a linear inhibition of pathway flux. We extrapolated the solid line to give a visual indication of the y-intercept (dotted line). A higher y-intercept indicates a greater excess capacity of CIV, and the [y-intercept – 1]/y-intercept represents the amount that that complex has to be inhibited before it begins affecting the overall combined pathways' flux (i.e., the excess capacity of the complex). In other words, the greater the excess capacity of a complex, the less chance of a decrease in overall respiration when that complex begins to lose its function.

Here, the significant differences in y-intercepts showed a higher apparent excess capacity of CIV in the L line compared to the E line (Fig. 13A-D; $P = 0.007$), but there was only a significant difference at day 1 (Fig. 13A, C; median y-intercept of 1.594 for the E line and 1.806 for the L line, $P = 0.003$). There was no difference between the lines at day 5 (Fig. 13B, D; 1.743 for the E line and 1.878 for the L line, $P = 0.380$). There was no effect of age in both beetle selection lines (Fig. 13A-D; $P = 0.066$). In comparing the slopes, there was again a significant effect of the selection line, with L line beetles presenting a higher CIV excess capacity than E line beetles (Fig. 13A-D; $P = 0.009$). This difference was observed between the lines specifically at day 1 (Fig. 13A, C; $P = 0.004$). Unlike for the y-intercepts, there was a significant increase in excess CIV capacity with age, but only in the E line (Fig. 13A, B; $P = 0.012$ for the E line, $P = 0.670$ for the L line).

There was no interaction between selection line and age in comparing both the y-intercepts and the slopes (Fig. 13A-D; $P = 0.095$ for y-intercepts and $P = 0.094$ for slopes).

When 25% of CIV was inhibited (Fig. 13E), the capacity of the combined NSPro pathways was more preserved in the L line compared to the E line at day 1 (95% vs 93% of overall NSPro flux in the L line vs E line; $P = 0.005$), but these differences were absent at day 5 (Fig. 13E; 96% vs 95%; $P = 0.320$). The same pattern was observed at 50% inhibition (Fig. 13F; 81% vs 76% in the L vs E lines at day 1, $P = 0.007$; and 82% vs 82% at day 5, $P = 0.807$). When looking at the effect of age, the impact of 25 and 50% inhibition of CIV excess was different in each beetle selection line. The E line was less affected by CIV inhibition at day 5 compared to day 1 at 25% of CIV inhibition (Fig. 13E; 96% vs 93% at days 5 vs 1, $P = 0.007$), and this was a trend at 50% inhibition (Fig. 13F; 82% vs 76%, $P = 0.052$). In the L line, there was no significant change with age at any of the percent inhibitions measured (Fig. 13E and F; 95% vs 95% at days 5 vs 1, $P = 0.979$ at 25% inhibition, and 82% vs 81%, $P = 0.442$ at 50% inhibition).

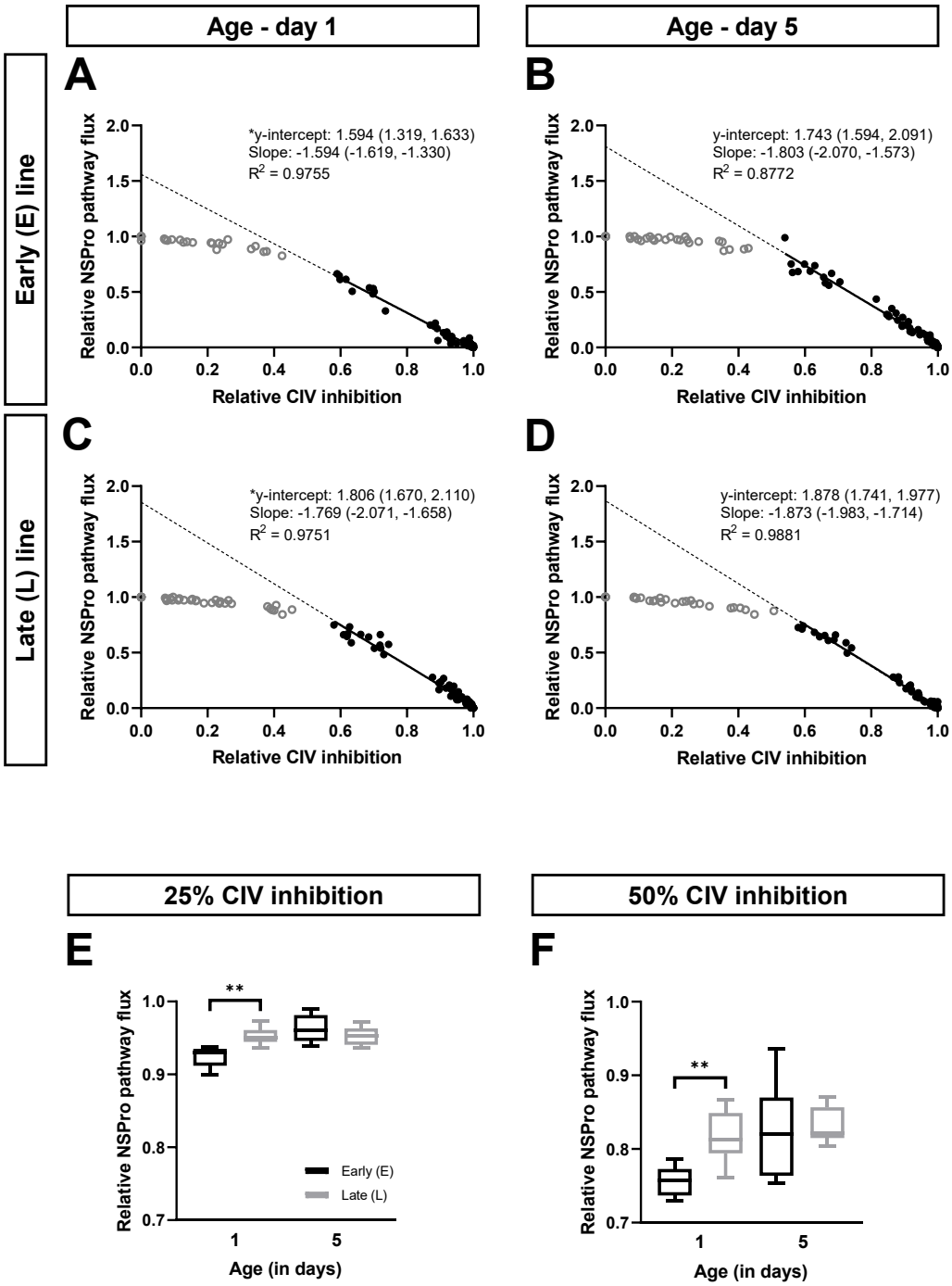

Figure 13: Effect of complex IV inhibition on maximal pathway flux. (A-D) The relative maximal pathway flux in the presence of NADH, succinate and proline (NSPro) is presented as a function of relative complex IV (CIV) inhibition using a sodium azide titration at days 1 (panels A and C) and 5 (panels B and D) in males of the early (E; panels A and B) and late (L; panels C and D) seed beetle selection lines. Dots represent the raw data plots. Data up to the threshold of inhibition are represented by open, grey circles, while data after the inflection point are represented by closed, black circles. The y-intercept represents the intercept of the linear regression of the data after the inflection

point with zero CIV inhibition. Y-intercepts are listed on the graphs as median (min, max) and represent the apparent excess CIV capacity. Graphs also display the slopes as median (min, max) as well as the goodness of fit (R^2). Data were analyzed using a two-way ANOVA and met the assumptions without undergoing any transformations. Two-way ANOVA results comparing y-intercepts are: $P = 0.007$ (the effect of selection line), $P = 0.066$ (the effect of age), and $P = 0.095$ (interaction). Significant differences between the y-intercepts of selection lines are denoted * ($P = 0.003$). (E-F) The relative NSPro flux at 25% (panel E) and 50% (panel F) CIV inhibition, at days 1 and 5 in males of the E and L lines. n = 5-7 at both ages and in both lines. Significant differences between the lines as the result of t-test statistical analyses are denoted ** ($P \leq 0.01$).

3.11 Quality of the mitochondria

LEAK state respiration (Fig. 14A, B) was measured with pyruvate, malate, and glutamate without the presence of ADP. LEAK was expressed as FCR, which is known as the coupling-control ratio: a LEAK value of 0 indicates a fully coupled system, whereas a LEAK value of 1 indicates a fully uncoupled system (Gnaiger, 2020). Our results show that most LEAK values are below 0.05, which is indicative of good coupling in *A. obtectus* mitochondria in both females (Fig. 14A) and males (Fig. 14B) and in both beetle lines. There were no significant differences between any of the parameters studied (i.e., age and line).

The cytochrome *c* effect indicates the integrity of the external mitochondrial membrane (Gnaiger, 2020). The cytochrome *c* effect significantly increased with age in both females and males; in females, an increase was observed in both lines between days 1 and 8 (Fig. 14C; $P < 0.001$ in the E line, $P = 0.021$ in the L line), and only in the E line between days 5 and 8 ($P = 0.009$). In males, there was an increase in the cytochrome *c* effect earlier on, notably between days 1 and 5 in both lines (Fig. 14D; $P < 0.001$ in the E line and $P = 0.005$ in the L line), but also between days 1 and 8 only in the E line ($P = 0.001$). The effect of longevity was only seen at day 8 in females (Fig. 14C, $P = 0.028$) but at days 1 and 5 in males (Fig. 14D, $P = 0.002$ and $P = 0.018$, respectively).

To avoid any bias induced by changes in outer membrane integrity, OXPHOS capacity values used for comparison between ages and lines were all taken after addition of exogenous cytochrome *c*.

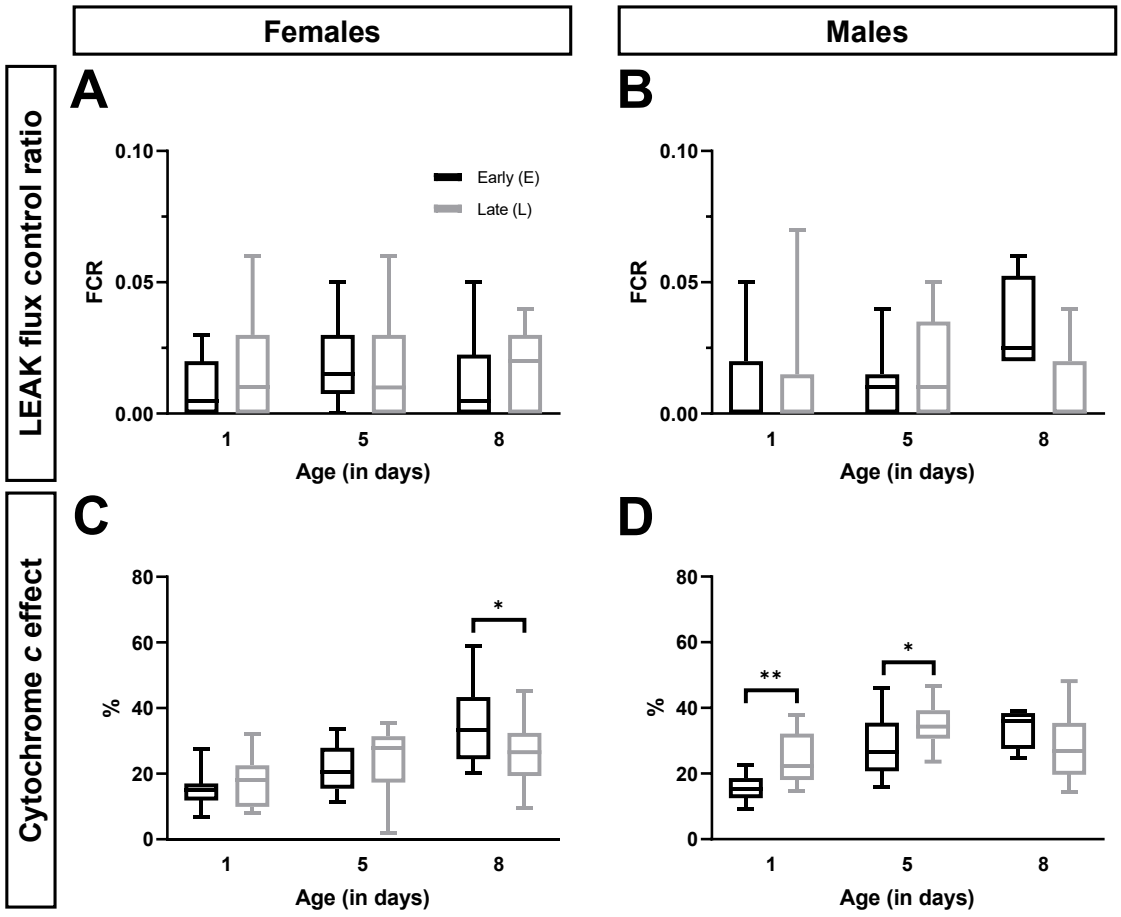

Figure 14: Indicators of mitochondrial quality. (A-B) The flux control ratio (FCR) for the LEAK state was measured in the presence of pyruvate, malate, and glutamate, before the addition of ADP and expressed as the maximal OXPHOS state in the presence of NADH, succinate and proline (with ADP and cytochrome *c*). (C-D) The cytochrome *c* effect is presented as a percentage (%) of increase in respiration following the addition of cytochrome *c* with respect to the NADH pathway in the OXPHOS state. Both the LEAK state and the cytochrome *c* effect were measured at days 1, 5, and 8. Data for female seed beetles are shown in panels A and C (n = 14-18 in the E line, 15-17 in the L line). Data for male seed beetles are shown in panels B and D (n = 14-16 for days 1 and 5, 4 for day 8 in the E line, 13 for all timepoints in the L line). Box plots indicate the minimum, 25th percentile, median, 75th percentile, and maximum. Data in all panels did not meet the assumptions of the two-way ANOVA, so the following tests were performed: one-way ANOVA (age effect within the L line in panels C and D), Kruskal-Wallis ANOVA on ranks (age effect within each line in panels A and B, within E line in panels C and D), t-test (line effect at days 1, 5, and 8 in panel C, days 5 and 8 in panel D), and Mann-Whitney rank sum test (line effect at days 1, 5, and 8 in panels A and B, day 1 in panel D). Significant differences between the beetle lines are denoted * ($P \leq 0.05$) and ** ($P \leq 0.01$).

4. DISCUSSION

In this study, we provide evidence of the connection between mitochondrial function and important differences in longevity in the E and L selection lines of *A. obtectus*. We observed that beetles of the L line, compared to the E line, had a decreased flux and contribution of the NADH pathway through CI, which was observed at early time points (days 1 and 5), and tended to have more differences in males compared to females. Furthermore, at day 1, males showed an increase in control by CI on overall flux. As a compensation for the decreased capacity of the NADH pathway through CI, L line beetles showed an increase in the contribution of the Succinate pathway through CII. These differences were present in both sexes, but males tended to have differences in earlier timepoints. L line beetles also displayed greater excess CIV capacity early in life compared to the E line at day 1 of age. Additionally, the ProDH pathway did not vary between the beetle selection lines, and both beetle lines had a very limited capacity to oxidize fatty acid substrates. So, these two neglected pathways (the ProDH pathway and the ETF pathway using fatty acid substrates) do not appear to play a role in the selection for lifespan in *A. obtectus*.

4.1 Decrease in the NADH pathway capacity associated with an increase in longevity

Our results pointed towards a reduction in CI being linked to increasing lifespan in the beetles. This is supported by (1) the lower contribution of the NADH pathway through CI to the maximal OXPHOS capacity in the L line compared to the E line, and (2) the higher control by CI in the L line compared to the E line. Our data supports other research demonstrating that CI disruption or

partial inhibition extends lifespan. First, lifespan extension was directly observed following RNAi of CI in *C. elegans* (Curran and Ruvkun, 2007; Dillin et al., 2002; Hamilton et al., 2005; Hansen et al., 2005; Labbadia et al., 2017; Rauthan et al., 2015; Rea et al., 2007; Yang and Hekimi, 2010b) and in *D. melanogaster* (Copeland et al., 2009; Owusu-Ansah et al., 2013). Another study saw lifespan extension after RNAi of ATP synthase subunit C, which suppressed CI activity in *C. elegans* (Xu et al., 2018). Second, inhibition of CI with rotenone was associated with an increase in longevity in the short-lived killifish *Nothobranchius furzeri* (Baumgart et al., 2016) and in *C. elegans* (Labbadia et al., 2017). In the killifish study, they first noticed that CI-linked genes were negatively correlated with lifespan: the short-lived killifish had a higher expression of CI genes than the longer-lived killifish. In the second part of their project, they administered low concentrations of rotenone to the short-lived killifish and found that their lifespan was extended by 15% (Baumgart et al., 2016). In *C. elegans*, Labbadia et al. (2017) administered low concentrations of rotenone until the late larval stage and saw increased survival following heat shock on day 2 of adulthood. Third, studies have shown a lower abundance of CI and/or its subunits in long-lived strains of mice (Miwa et al., 2014) and *C. elegans* (Munkácsy and Rea, 2014).

Interestingly, a previous study measured the activity of the various complexes in E and L line beetles. They did not find a difference in CI activity between the lines, but noted an increase in CIII activity in the L line compared to the E line (Đorđević et al., 2017). The difference between their results and ours could be explained by various differences in measurements between the studies; their activities were expressed per mg of protein, measured only at day 1, and with assays performed on frozen mitochondria, without the functionality of the global OXPHOS process. In contrast, our data localized the defect to the NADH pathway through CI in the L line compared to the E line by performing experiments on functional mitochondria, measuring the entire OXPHOS

process using a polarographic assay, and working on intact mitochondria and closer to the conditions of the live animal (Lemieux and Hoppel, 2009). Furthermore, using the titration curves of the CI inhibitor, rotenone, we can support that the defect noted in the NADH pathway measured with pyruvate, malate and glutamate as substrates was at least in part due to a decrease in CI, and not in other steps involved in the NADH pathway (such as pyruvate dehydrogenase, transaminase, and substrate transporters). Our titration curves showed that L line beetles, compared to E line beetles, lack an excess of CI, since inhibition by rotenone exerted an earlier and more significant effect on the global pathway flux with NADH, Succinate, and Proline pathways active. Notably, this decrease in CI capacity in the L line compared to the E line better agrees with another previous study in these beetle selection lines, that showed that exposure to low doses of the CI inhibitor, tebufenpyrad, in 1-day-old short-lived (E line) seed beetles extended their lifespan by nearly 15% (Jovanović et al., 2014). The results presented here and by Jovanović et al. (2014) demonstrate that the decrease in CI in the long-lived line is not a coincidence, but is instead a mitochondrial adjustment involved in lifespan extension.

4.2 No change in the Proline dehydrogenase (ProDH) pathway associated with longevity, but a decrease associated with age

Whereas other sources have suggested an increase in proline metabolism to be involved in controlling lifespan in *S. cerevisiae* (Mukai et al., 2019; Nishimura et al., 2021) and *C. elegans* (Edwards et al., 2015; Pang and Curran, 2014), our results do not support this change in *A. obtectus*, as both lines showed the same capacity of the ProDH pathway when expressed in FCR and in Flux per unit of CS activity. The two beetle selection lines, however, have an important

capacity to process OXPHOS using proline as a substrate. Interestingly, it could be advantageous for the L line to have an increase in the capacity of the Succinate pathway rather than the ProDH pathway because the ProDH pathway already provides an important energy source for OXPHOS and has previously been reported to promote aging by producing large amounts of ROS via an upregulation of ProDH by p53 (Nagano et al., 2017). Additionally, a cross-talk between the ProDH and Succinate pathways has been previously detected (Hancock et al., 2016).

Furthermore, the contribution of the ProDH pathway (in FCR and in Flux per unit of CS activity) decreased with age in both sexes. This supports earlier data on *D. melanogaster* which showed a decrease in proline oxidation, normalized to mitochondrial protein content, with age (Ferguson et al., 2005). Proline is also associated with insect flight muscle (Gäde and Auerswald, 2002; Teulier et al., 2016). As a result, the decrease in overall contribution of proline with age could be a proxy for insect motility, since aging insects become less physically active and less prone to flying (Lane et al., 2014; Le Bourg and Minois, 1999; Miller et al., 2008; Simon et al., 2006; Tofilski, 2000).

4.3 Unexpectedly low capacity to oxidize fatty acids in both beetle lines

Our data for *A. obtectus* showed a low capability of using fatty acid substrates for OXPHOS compared to substrates used by the NADH, Succinate, or Proline pathways. We observed this with three different chain lengths of fatty acids: the long chain fatty acid palmitoylcarnitine (medians of 11% and 16% of the NADH pathway in E and L lines, respectively), the medium chain fatty acid octanoylcarnitine (9% and 11% of the NADH pathway in E and L lines, respectively) and the short chain fatty acid acetylcarnitine (10% of the NADH pathway in L; data not shown). Our data contradicts suggestions made based on respiratory quotients, which are the ratio of CO_2 produced

to O_2 consumed. The respiratory quotient reflects which macronutrients are used for metabolism. Animals with a low respiratory quotient (around 0.7), like beetles (Immonen et al., 2016; Wightman, 1978) and even the seed beetle selection lines used in our study (Arnqvist et al., 2017), were thought to almost exclusively use lipids as an energy source (Kleiber, 1961). In contrast, our data suggest that even during starvation, *A. obtectus* do not oxidize fatty acids to produce energy. Furthermore, the observation that E line beetles have a slightly higher respiratory quotient compared to L line beetles (Arnqvist et al., 2017) cannot be due to a difference in the capacity to oxidize fatty acids, as our results showed a similar, very limited capacity to produce energy from fatty acids in both selection lines.

There are two potential explanations for this low capacity to oxidize fatty acids in the beetles. The first explanation is that the mobilization of fuel in the fat bodies is not directly oxidized as fatty acids but shuttled in the form of proline, as previously suggested for insects (Arrese and Soulages, 2010; Bursell, 1977; Bursell, 1981; Gäde and Auerswald, 2002). This process is called the proline-alanine cycle, which ultimately transforms fatty acid reserves and alanine into proline (Gäde and Auerswald, 2002). In the Colorado potato beetle (*Leptinotarsa decemlineata*), which oxidizes proline to fuel flight, a concomitant utilization of glucose occurs to produce pyruvate, and allows the proline-alanine cycle to run (Gäde and Auerswald, 2002). In *A. obtectus*, as feeding is absent in the adult stage, the pyruvate needed for the proline-alanine cycle is likely supplied by stored lipids. And again, our data showed that *A. obtectus* use proline as an important energy source for OXPHOS and not fatty acids, emphasizing the possible importance of the proline-alanine cycle, fueled by fatty acids, in these beetles.

The second possible explanation for the lack of FAO in our seed beetles is that a respiratory quotient lower than 0.7 can occur when ketone bodies are being oxidized in starvation conditions

(Matarese, 1997; Schutz and Ravussin, 1980). Seed beetles can have an exceptionally low respiratory quotient (Arnqvist et al., 2017), and even a lower respiratory quotient than the theoretical minimum of 0.7 predicted under pure FAO (Kleiber, 1961). This low respiratory quotient (lower than or close to 0.7) is common in insects (Arnqvist et al., 2017; Blossman-Myer and Burggren, 2010; Damcevski et al., 1998; Devries et al., 2013; DeVries et al., 2015; Rouland et al., 1993; Vogt and Appel, 1999). Furthermore, the use of ketone bodies as an energy source during starvation has been previously observed in insects (Bailey and Horne, 1972; Niitepõld et al., 2022). In monarch butterflies, it has been suggested that lipids are used as an energy source for flight when the animals are fed (respiratory quotient of 0.73; Niitepõld et al., 2022). However, when food-deprived, the animals' respiratory quotient drops even further, indicating a potential switch to alternative energy sources such as ketone bodies (Niitepõld et al., 2022). There is also evidence of ketone bodies in the desert locust (*Schistocerca gregaria*), as lipid reserves become depleted when the insects fly or starve (Bailey and Horne, 1972). Together, our data indirectly suggest that the low respiratory quotient in *A. obtectus* (Arnqvist et al., 2017) could be explained by a higher use of ketone bodies as an energy source instead of fatty acids. This pathway of energy production has never been measured in this beetle model, so warrants future studies to address this possible explanation for low FAO.

4.4 Increase in the Succinate dehydrogenase pathway compensates for the loss of the NADH pathway in long-lived beetles

Our results in *A. obtectus* showed a higher contribution of the Succinate pathway (both in FCR and in Flux per unit of CS activity) in long-lived beetles as a way to counterbalance the loss of electrons entering through CI. Other animal models with a defect in CI also showed a compensatory mechanism favoring an increase in the capacity of CII, e.g. following a mutation in a subunit of CI (*gas-1*) in *C. elegans* (Kayser et al., 2001; Kayser et al., 2004) and following the negative effect of a high-fat diet on CI in *D. melanogaster* (Cormier et al., 2019). In a model of human cardiomyocyte metabolism, a simulation of CI deficiency was associated with the smallest reduction in ATP production, in part due to multiple potential compensatory mechanisms, including sources other than succinate, such as proline, glycerophosphate, and FAO (Zieliński et al., 2016). This predicted metabolic flexibility may explain why isolated CI disorders represent a high proportion of respiratory chain diseases (Kirby et al., 1999; Loeffen et al., 2000) – alternate, compensating metabolic pathways would give patients the highest chance of survival (Zieliński et al., 2016). In contrast, CII deficiencies are very rare and account for only about 1-2% of respiratory system disorders (Loeffen et al., 2000; Rustin et al., 1993). Simulations of mitochondrial ETS dysfunction suggested a larger effect of a CII deficiency on ATP production and the lack of options for compensatory mechanisms to overcome it (Zieliński et al., 2016).

Our respiration data with proline and various fatty acids did not vary between the lines, and FAO was minimal, so our data does not suggest that these pathways were used to compensate for the CI defect in the L line. The compensation occurs through CII, which is typically the complex where its decrease is not associated with an improvement in lifespan in *C. elegans* (Hamilton et al., 2005;

Ichimiya et al., 2002; Kuang and Ebert, 2012; Yang and Hekimi, 2010b). In contrast, all other defects of complexes have been associated with an increase in lifespan in various species including *C. elegans*, *Drosophila*, zebrafish, and mice: CI (see above; Baumgart et al., 2016; Copeland et al., 2009; Curran and Ruvkun, 2007; Hamilton et al., 2005; Labbadia et al., 2017; Owusu-Ansah et al., 2013; Rauthan et al., 2015; Rea et al., 2007; Yang and Hekimi, 2010b), CIII (Copeland et al., 2009; Feng et al., 2001; Labbadia et al., 2017; Yang and Hekimi, 2010b), CIV (Copeland et al., 2009; Dell'agnello et al., 2007; Dillin et al., 2002; Durieux et al., 2011; Hamilton et al., 2005; Hansen et al., 2005; Labbadia et al., 2017; Rea et al., 2007), and/or ATP synthase (Copeland et al., 2009; Curran and Ruvkun, 2007; Dillin et al., 2002; Hamilton et al., 2005; Hansen et al., 2005; Rea et al., 2007; Xu et al., 2018). By increasing the Succinate pathway through CII to compensate for the reduction in the NADH pathway through CI, L line beetles preserve energy production while eliminating the chance for CII to negatively affect lifespan.

4.5 Larger excess of CIV capacity in long-lived beetles and an increase in contribution of CIV activity with age in both selection lines

Another result in our study was the change in proportion of CIV compared to the overall (NADH, Succinate and Proline combined) pathway flux between the lines. In males only, CIV had a higher activity in FCR and Flux over CS activity in the L line compared to the E line. The CIV inhibitor titrations in males also showed more CIV excess in the L line compared to the E line at a young age (day 1). So, in the L line, the excess CIV capacity is already higher at day 1 (y-intercept = 1.8) compared to the E line (1.6), and both lines are equivalent at day 5. These results, in conjunction with the lower CI capacity in L line beetles early in life, seem to suggest that the presence of an

excess in CIV in the L line at day 1 is secondary to the adjustment in CI capacity; a reduction in CI capacity in L line beetles automatically led to a larger CIV excess capacity early in life, since a lesser proportion of CIV became necessary. And after the decrease in the NADH pathway at day 1, there is a secondary adjustment of CIV, leading to a similar excess capacity in both lines at day 5. It can therefore be suggested that in these beetles, CIV itself may not be important for lifespan extension. In *A. obtectus*, the higher CIV excess in L line beetles at day 1 rather emphasizes the importance of CI in influencing lifespan in these beetles.

This connection between CI and CIV also alludes to the presence of supercomplexes in *A. obtectus*. Supercomplex assemblies tend to involve two or three of CI, CIII, and CIV. And some studies suggest that in order to function properly, CI depends on forming supercomplexes with CIII and CIV (Acín-Pérez et al., 2004; Suthammarak et al., 2009). Furthermore, CII has been suggested to be less likely, or not at all, involved in supercomplexes in various marine bivalve species (Rodríguez et al., 2022), in *C. elegans* (Suthammarak et al., 2009), in cardioblast cells (Jang and Javadov, 2018), and in humans (Guo et al., 2017). Furthermore, it was recently found that the complexity of supercomplexes was positively correlated with lifespan, with the extremely long-lived bivalve, *Arctica islandica* (maximum documented lifespan of 507 years), having supercomplexes that consisted more of CI and CIV, as well as ATP synthase (Rodríguez et al., 2022). So, our results show a coordinate adjustment of CI and CIV but a contrasting adjustment of CII in particularly the L line which could be related to the importance of preserving supercomplexes. Further studies are needed to evaluate the association between CI and CIV in these beetle selection lines.

4.6 Less mitochondrial content associated with longevity

The pace-of-life hypothesis suggests that longevity is affected by the rate of physiological functions such as the metabolic rate (Martin et al., 2006; Réale et al., 2010; Ricklefs and Wikelski, 2002; Wikelski et al., 2003). This hypothesis is in agreement with our results showing a higher indicator of mitochondrial content (at days 1 and 5) in the short-lived (E) line compared to the long-lived (L) line. Other results also are in agreement with this hypothesis: (1) our results showed that E line beetles generally had a higher combined pathway flux (Fig. 8) than L line beetles when measured in Flux per mass, (2) on the same animal model as our study, E line beetles have been shown to have a markedly higher (18%) metabolic rate compared to L line beetles (Arnqvist et al., 2017), (3) a study on *C. elegans* found that individuals with a longer lifespan exhibit a reduced metabolic rate (Sedensky and Morgan, 2006), and (4) less mitochondrial content in long-lived animals was also seen in the naked mole rat, compared to mice (Munro et al., 2019). However, there are also contrasting results, such as those of marine bivalves with varying longevities, where the long-lived marine bivalve *A. islandica* had more CS than shorter-lived bivalves (Rodríguez et al., 2021). There are various explanations for this contrast with the results presented here: (1) the study on bivalves compared different species with differing longevities, (2) the ages of the bivalves were not specified, and (3) hypoxia could play a role since bivalves burrow in sand.

4.7 Potential effects of modified OXPHOS function on ROS production

Our data show, in the long-lived line, compared to the short-lived line, (1) a lower contribution of the NADH pathway through CI, (2) a higher contribution of the Succinate pathway through CII, (3) less mitochondrial content, and (4) a higher CIV excess capacity. This is interesting, as all these changes have been previously suggested to be linked to a reduction in ROS production. First, CI, and more specifically its Q-binding site or iron-sulfur clusters, is a well-recognized contributor to ROS production (Herrero and Barja, 2000; Lambert and Brand, 2004). In fact, CI is considered as the main site of ROS production in mitochondria (Brand, 2010; Kowaltowski et al., 2009). Second, ROS production from CII is generally recognized as minimal (Miwa et al., 2014; Muller et al., 2008; St-Pierre et al., 2002), and downregulation of CII levels and/or activity generally results in lifespan shortening (Huang and Lemire, 2009; Ishii et al., 1998; Pujol et al., 2013; Szeto et al., 2007; Walker et al., 2006). Third, as mitochondria are major ROS producers, less mitochondrial content could be associated with lower ROS production (Kogot-Levin et al., 2016; Yamamori et al., 2012). Fourth, as reducing CIV excess enhances the production of ROS from certain upstream sites in the ETS, mostly from CI (Chen et al., 2003), it is likely that an increased excess of CIV has the advantage of reducing the risk of ROS production by the ETS.

Interestingly, there is another way to see things that should also be evaluated. A slight reduction in some mitochondrial complexes' activity (including CI) early in life can also generate mitochondrial stress, favor ROS production, and activate mechanisms that slow aging later in life. It was previously suggested that long-lived animals needed an increase in ROS early in life in order to activate lifespan-extending cell-signaling pathways. This was first called the hormetic effect which was defined as repeated, short-lasting and nonlethal stressors that activate stress

response mechanisms, increase stress resistance, and extend lifespan (Masoro, 2006; Minois, 2000; Neafsey, 1990; Rattan, 2000; Rattan, 2001; Rattan, 2004; Verbeke et al., 2000). This effect, when connected to a burst in ROS production in mitochondria, is termed mitohormesis (Ristow, 2014; Ristow and Zarse, 2010; Schulz et al., 2007; Tapia, 2006; Yun and Finkel, 2014). For example, in *C. elegans* exposed for 48 hours to a molecule impairing glucose metabolism, there is a resulting spike in ROS production (3-fold), an increase in resistance to the pro-oxidant paraquat, and an increase in longevity (Schulz et al., 2007). Another example occurs in the model *D. melanogaster*, where temporary, short-term (24 hours) knocked-down expression of a CI component resulted in an increase in ROS levels and an increase in lifespan (Owusu-Ansah et al., 2013). More recently, the increase in longevity related to a spike in ROS production early in life has been linked with activation of hypoxia-inducible factor 1 (HIF-1; Hwang and Lee, 2011; Pujol et al., 2013) and the mitochondrial unfolded protein response (UPRmt; Labbadia et al., 2017; Owusu-Ansah et al., 2013; Rauthan et al., 2015).

An additional factor involved in the mitohormesis effect is that a preserved excess of ROS later in life, following the initial burst early in life, could hinder lifespan extension by exceeding the cell's defense mechanisms (Huang and Lemire, 2009). With this in mind, there may be a threshold effect where ROS have to be maintained at lower levels to prevent excess damage. In order to balance ROS amounts that produce lifespan extension and prevent overall oxidative damage, it is important for organisms to have proper antioxidant defenses (Huang and Lemire, 2009; Munro et al., 2019; Yang and Hekimi, 2010a). In our experimental model, L line beetles have a higher superoxide dismutase activity at old (10 days) age compared to E line beetles (Seslija et al., 1999), and generally are more resistant to oxidative stress (Lazarević et al., 2013; Seslija et al., 1999). In the well-recognized long-lived naked mole rat, there is also an increase in antioxidant defenses

compared to mice (Munro et al., 2019). The extremely long-lived marine bivalve, *A. islandica*, also presents higher levels of catalase activity (Abele et al., 2009) and a high capacity to remove H_2O_2 (Munro et al., 2023), which explains their unexpectedly low H_2O_2 efflux compared to short-lived bivalves (Munro et al., 2013).

Our data support the mitohormetic effect when looking at the time points where most of the mitochondrial differences occur: at earlier time points, i.e., days 1 and 5. Earlier differences between the *A. obtectus* lines support the importance of an increased mitochondrial stress early in life (here, conceivably the decrease in the NADH pathway in long-lived beetles) in order to potentially offer more stress resistance later in life and ultimately extend lifespan. Furthermore, L line beetles have lower catalase activity compared to E line beetles at day 1 (Seslija et al., 1999), which could be another potential mechanism that favors higher ROS production early in life in the L line and the mitohormetic effect. Future experiments on ROS production and ROS management associated with the various OXPHOS pathways would elucidate the role of ROS and the importance of the mitohormetic effect and/or the threshold effect in these beetles.

5. CONCLUSION

5.1 Significance

Our study looked at various metabolic pathways and pathway control and emphasizes the importance in understanding the specific changes in integrated mitochondrial function that are connected to lifespan. Through our use of E and L lines of *A. obtectus*, which have been selected for reproduction and longevity since 1986, we determined mitochondrial differences between differing lifespans within the same animal species. Additionally, we compared females and males and found that males tended to have earlier differences than females and more differences linked to longevity. This presence of more differences in males suggests the Mother's curse hypothesis (Gemmell et al., 2004) which supports previous work on these seed beetle lines where mated males had more significant costs to longevity (Đorđević et al., 2015).

In long-lived beetles, there was a lower use of the NADH pathway and a higher control on overall flux by CI, pointing to CI as a possible regulator of lifespan in these beetles. L line beetles also had a greater excess capacity of CIV than E line beetles early in life, but this seems to be a secondary adjustment to the change in the NADH pathway and overall flux control by CI. This further supports the importance of CI in affecting lifespan in these beetles. L line beetles additionally had a higher contribution of the Succinate pathway than E line beetles. This study not only evaluated differences in the well-recognized NADH and Succinate pathways, but also looked at understudied pathways, notably the ProDH pathway and FAO. The ProDH pathway showed no difference between the lines. Despite conditions of starvation, beetles of both lines did not use FAO as an energy source, highlighting the need to study other, less-understood metabolic

pathways in order to determine their non-carbohydrate energy sources. Taken together, this study further supports the link between CI and longevity in a proven model of longevity.

5.3 Limitations and future directions

Our laboratory is currently investigating or is planning to start investigating the following, in order to strengthen the interpretation of our findings in *A. obtectus*:

1. We have already begun investigating the metabolite profiles in both selection lines, both sexes, and at all three time points using mass spectrometry. I went to Dr. Blier's research lab in Rimouski to prepare the samples for this analysis. We are awaiting the final set of results and will begin analysis in the upcoming weeks. Metabolomic profiles can be linked to longevity in various models, such as in humans (Cheng et al., 2015) and naked mole rats (Lewis et al., 2018; Viltard et al., 2019). Lower levels of citric acid cycle intermediates (Cheng et al., 2015), lower levels of amino acids (Lewis et al., 2018; Viltard et al., 2019), and lower levels of fatty acids (Lewis et al., 2018) have been shown to be associated with longevity. Differences in metabolite concentrations could strengthen our evidence of the involvement of the CI in determining longevity and could also suggest other important metabolites for longevity in seed beetles.

2. To evaluate differences in fatty acid composition of mitochondrial and cellular membranes, we are using gas chromatography. The degree of cellular and mitochondrial membrane fatty acid unsaturation has been suggested as an indicator of lifespan (Barja, 2014; Pamplona et al., 2002). Long-lived animals tend to have a lower fatty acid double bond

index and a lower peroxidizability index, which could help maintain membrane fluidity while reducing membrane sensitivity to peroxidation (Barja, 2014). Already half of the samples that I prepared have been run, but they have yet to be analyzed. The remaining samples have been collected and are awaiting lipid extraction. We also plan on evaluating the fatty acid composition of lipid storage in the body of whole beetles to determine if other fatty acids may be important for energy production. We then plan on testing these lipids using high-resolution respirometry. Lipid extraction from whole bodies has occurred for all samples, and the samples are ready to be run using mass spectrometry.

3. We will shortly begin measuring ROS production of specific OXPHOS pathways in the beetle lines using High-Resolution FluoRespirometry. We are also planning to evaluate oxidative damage and oxidative stress defense mechanisms. These experiments could provide evidence of ROS' level of involvement in determining the lifespan in the selection lines of *A. obtectus*.

4. Using high-resolution respirometry, we plan to evaluate ketone body metabolism as a potential energy source in *A. obtectus*. Since *A. obtectus* do not eat after eclosion, there is a lack of carbohydrate energy sources. When other substrates are not available, ketone bodies are generated from fatty acids and become important for energy production (Longo and Mattson, 2014). Additionally, ketone metabolism has been shown to extend lifespan (Veech et al., 2017) and be involved in an increased healthspan (Lin et al., 2015).

5. FAO and mitochondrial control by specific complexes were only studied in males. Future high-resolution respirometry experiments could be done on females to then compare differences in FAO and in mitochondrial ETS control between the sexes.

6. Executing additional experiments on an earlier time point, notably within the first 2 hours after eclosion from the bean, could support our hypothesis that earlier mitochondrial changes could promote longevity. Within the first 2 hours after eclosion, seed beetles do not begin mating, so it is possible that final reproductive development occurs at this time.

7. We did not control for beetle mating status. It is possible that some of the differences seen with longevity and/or age are connected to the mating status, or that the mating status would have added more clarity to our results. Since very few males lived to or surpassed 8 days of age (no data presented), we can deduce that most of our animals were mated. The mating status has been shown to affect the longevity of both males and females in both lines (Đorđević et al., 2015).

8. We are beginning a collaboration with Dr. Thomas Simmen (Department of Cellular Biology, University of Alberta) to run Western blots investigating the activation of the UPRmt pathway in *A. obtectus*. Activation of the UPRmt response has been associated with animal longevity in *C. elegans* (Labbadia et al., 2017; Pujol et al., 2013; Rauthan et al., 2015; Tian et al., 2016; Wu et al., 2018; Xin et al., 2022) and *Drosophila* (Owusu-Ansah et al., 2013). Expression levels of HSP-6 (Labbadia et al., 2017; Xin et al., 2022), HSP-16 (Labbadia et al., 2017), and ATFS-1 (Wu et al., 2018) proteins increased in *C. elegans* with longer lifespans, so we would like to specifically look at these proteins in *A. obtectus*.

9. To determine the presence and components of supercomplexes, we can run blue native polyacrylamide gel electrophoresis. Supercomplex organization of the ETS has been suggested to play a role in the longevity of marine bivalves (Rodríguez et al., 2022).

REFERENCES

Abele, D., Brey, T. and Philipp, E. (2009). Bivalve models of aging and the determination of molluscan lifespans. *Exp Gerontol* **44**, 307-15.

Acín-Pérez, R., Bayona-Bafaluy, M. P., Fernández-Silva, P., Moreno-Loshuertos, R., Pérez-Martos, A., Bruno, C., Moraes, C. T. and Enríquez, J. A. (2004). Respiratory complex III is required to maintain complex I in mammalian mitochondria. *Mol Cell* **13**, 805-15.

Akbari, M., Kirkwood, T. B. L. and Bohr, V. A. (2019). Mitochondria in the signaling pathways that control longevity and health span. *Ageing Res Rev* **54**, 100940.

Alaux, C., Sinha, S., Hasadsri, L., Hunt, G. J., Guzmán-Novoa, E., DeGrandi-Hoffman, G., Uribe-Rubio, J. L., Southey, B. R., Rodriguez-Zas, S. and Robinson, G. E. (2009). Honey bee aggression supports a link between gene regulation and behavioral evolution. *Proc Natl Acad Sci U S A* **106**, 15400-5.

Arnqvist, G., Stojković, B., Rönn, J. L. and Immonen, E. (2017). The pace-of-life: A sex-specific link between metabolic rate and life history in bean beetles. *Funct. Ecol.* **31**, 2299-2309.

Arrese, E. L. and Soulages, J. L. (2010). Insect fat body: energy, metabolism, and regulation. *Annu Rev Entomol* **55**, 207-25.

Bailey, E. and Horne, J. A. (1972). The role of ketone bodies in the metabolism of the adult desert locust. *Biochem J* **128**, 79p.

Balaban, R. S., Nemoto, S. and Finkel, T. (2005). Mitochondria, oxidants, and aging. *Cell* **120**, 483-95.

Ballard, J. W., Katewa, S. D., Melvin, R. G. and Chan, G. (2007). Comparative analysis of mitochondrial genotype and aging. *Ann N Y Acad Sci* **1114**, 93-106.

Barja, G. (2014). The mitochondrial free radical theory of aging. *Prog Mol Biol Transl Sci* **127**, 1-27.

Barrientos, A., Casademont, J., Rötig, A., Miró, O., Urbano-Márquez, A., Rustin, P. and Cardellach, F. (1996). Absence of relationship between the level of electron transport chain activities and aging in human skeletal muscle. *Biochem. Biophys. Res. Commun.*

Baumgart, M., Priebe, S., Groth, M., Hartmann, N., Menzel, U., Pandolfini, L., Koch, P., Felder, M., Ristow, M., Englert, C. et al. (2016). Longitudinal RNA-seq analysis of vertebrate aging identifies mitochondrial complex I as a small-molecule-sensitive modifier of lifespan. *Cell Syst* **2**, 122-32.

Bénit, P., Slama, A., Cartault, F., Giurgea, I., Chretien, D., Lebon, S., Marsac, C., Munnich, A., Rötig, A. and Rustin, P. (2004). Mutant NDUFS3 subunit of mitochondrial complex I causes Leigh syndrome. *J Med Genet* **41**, 14-7.

Beyer, R. E., Starnes, J. W., Edington, D. W., Lipton, R. J., Compton, R. T. r. and Kwasman, M. A. (1984). Exercise-induced reversal of age-related declines of oxidative reactions, mitochondrial yield, and flavins in skeletal muscle of the rat. *Mech. Ageing Dev.* **24**, 309-323.

Blier, P. U., Abele, D., Munro, D., Degletagne, C., Rodriguez, E. and Hagen, T. (2017). What modulates animal longevity? Fast and slow aging in bivalves as a model for the study of lifespan. *Semin. Cell Dev. Biol.* **70**, 130-140.

Blossman-Myer, B. L. and Burggren, W. W. (2010). Metabolic allometry during development and metamorphosis of the silkworm *Bombyx mori*: analyses, patterns, and mechanisms. *Physiol Biochem Zool* **83**, 215-31.

Boushel, R., Gnaiger, E., Schjerling, P., Skovbro, M., Kraunsoe, R. and Flemming, D. (2007). Patients with type 2 diabetes have normal mitochondrial function in skeletal muscle. *Diabetologia* **50**, 790-796.

Boveris, A. and Navarro, A. (2008). Brain mitochondrial dysfunction in aging. *IUBMB Life* **60**, 308-314.

Brand, M. D. (2010). The sites and topology of mitochondrial superoxide production. *Exp. Gerontol.* **45**, 466-472.

Bratic, I. and Trifunovic, A. (2010). Mitochondrial energy metabolism and ageing. *Biochim Biophys Acta* **1797**, 961-7.

Buffenstein, R., Edrey, Y. H., Yang, T. and Mele, J. (2008). The oxidative stress theory of aging: embattled or invincible? Insights from non-traditional model organisms. *Age (Dordr)* **30**, 99-109.

Burman, J. L., Itsara, L. S., Kayser, E. B., Suthammarak, W., Wang, A. M., Kaeberlein, M., Sedensky, M. M., Morgan, P. G. and Pallanck, L. J. (2014). A *Drosophila* model of mitochondrial disease caused by a complex I mutation that uncouples proton pumping from electron transfer. *Dis Model Mech* **7**, 1165-74.

Bursell, E. (1977). Synthesis of proline by fat body of the tsetse fly (*Glossina morsitans*): metabolic pathways. *Insect Biochem.* **7**, 427-434.

Bursell, E. (1981). The role of proline in energy metabolism. In *Energy metabolism in insects*, (ed. R. Downer), pp. 135-54. New York: Plenum.

Cai, Y., Song, W., Li, J., Jing, Y., Liang, C., Zhang, L., Zhang, X., Zhang, W., Liu, B., An, Y. et al. (2022). The landscape of aging. *Sci China Life Sci* **65**, 2354-2454.

Campuzano, V., Montermini, L., Moltò, M. D., Pianese, L., Cossée, M., Cavalcanti, F., Monros, E., Rodius, F., Duclos, F., Monticelli, A. et al. (1996). Friedreich's ataxia: autosomal recessive disease caused by an intronic GAA triplet repeat expansion. *Science* **271**, 1423-7.

Castelluccio, C., Baracca, A., Fato, R., Pallotti, F., Maranesi, M., Barzanti, V., Gorini, A., Villa, R. F., Castelli, G. P., Marchetti, M. et al. (1994). Mitochondrial activities of rat heart during ageing. *Mech. Ageing Dev.* **76**, 73-88.

Chen, Q., Vazquez, E. J., Moghaddas, S., Hoppel, C. L. and Lesnefsky, E. J. (2003). Production of reactive oxygen species by mitochondria: central role of complex III. *J. Biol. Chem.* **278**, 36027-36031.

Cheng, S., Larson, M. G., McCabe, E. L., Murabito, J. M., Rhee, E. P., Ho, J. E., Jacques, P. F., Ghorbani, A., Magnusson, M., Souza, A. L. et al. (2015). Distinct metabolomic signatures are associated with longevity in humans. *Nat Commun* **6**, 6791.

Choksi, K. B., Nuss, J. E., Deford, J. H. and Papaconstantinou, J. (2008). Age-related alterations in oxidatively damaged proteins of mouse skeletal muscle mitochondrial electron transport chain complexes. *Free Radic. Biol. Med.* **45**, 826-838.

Cocco, T., Sgobbo, P., Clemente, M., Lopriore, B., Grattagliano, I., Di Paola, M. and Villani, G. (2005). Tissue-specific changes of mitochondrial functions in aged rats: effect of a long-term dietary treatment with N-acetylcysteine. *Free Radic. Biol. Med.* **38**, 796-805.

Copeland, J. M., Cho, J., Lo, T., Jr., Hur, J. H., Bahadorani, S., Arabyan, T., Rabie, J., Soh, J. and Walker, D. W. (2009). Extension of *Drosophila* life span by RNAi of the mitochondrial respiratory chain. *Curr Biol* **19**, 1591-8.

Cormier, R. P. J., Champigny, C. M., Simard, C. J., St-Coeur, P. D. and Pichaud, N. (2019). Dynamic mitochondrial responses to a high-fat diet in *Drosophila melanogaster*. *Sci Rep* **9**, 4531.

Curran, S. P. and Ruvkun, G. (2007). Lifespan regulation by evolutionarily conserved genes essential for viability. *PLoS Genet* **3**, e56.

Damcevski, K., Annis, P. and Waterford, C. (1998). Effect of grain on apparent respiration of adult stored-product Coleoptera in an air-tight system: Implications for fumigant testing. *J. Stored Prod. Res.* **34**, 331-339.

Darnold, J. R., Vorbeck, M. L. and Martin, A. P. (1990). Effect of aging on the oxidative phosphorylation pathway. *Mech. Ageing Dev.* **53**, 157-167.

Dell'agnello, C., Leo, S., Agostino, A., Szabadkai, G., Tiveron, C., Zulian, A., Prelle, A., Roubertoux, P., Rizzuto, R. and Zeviani, M. (2007). Increased longevity and refractoriness to Ca(2+)-dependent neurodegeneration in Surf1 knockout mice. *Hum. Mol. Genet.* **16**, 431-44.

Devries, Z. C., Kells, S. A. and Appel, A. G. (2013). Standard metabolic rate of the bed bug, Cimex lectularius: effects of temperature, mass, and life stage. *J Insect Physiol* **59**, 1133-9.

DeVries, Z. C., Kells, S. A. and Appel, A. G. (2015). Effects of starvation and molting on the metabolic rate of the bed bug (Cimex lectularius L.). *Physiol Biochem Zool* **88**, 53-65.

Dillin, A., Hsu, A. L., Arantes-Oliveira, N., Lehrer-Graiwer, J., Hsin, H., Fraser, A. G., Kamath, R. S., Ahringer, J. and Kenyon, C. (2002). Rates of behavior and aging specified by mitochondrial function during development. *Science* **298**, 2398-401.

Đorđević, M., Savković, U., Lazarević, J., Tucić, N. and Stojković, B. (2015). Intergenomic interactions in hybrids between short-lived and long-lived lines of a seed beetle: analyses of life history traits. *Evol. Biol.* **42**, 461-72.

Đorđević, M., Stojković, B., Savković, U., Immonen, E., Tucić, N., Lazarević, J. and Arnqvist, G. (2017). Sex-specific mitonuclear epistasis and the evolution of mitochondrial bioenergetics, ageing, and life history in seed beetles. *Evolution* **71**, 274-288.

Durieux, J., Wolff, S. and Dillin, A. (2011). The cell-non-autonomous nature of electron transport chain-mediated longevity. *Cell* **144**, 79-91.

Edwards, C., Canfield, J., Copes, N., Brito, A., Rehan, M., Lipps, D., Brunquell, J., Westerheide, S. D. and Bradshaw, P. C. (2015). Mechanisms of amino acid-mediated lifespan extension in *Caenorhabditis elegans*. *BMC Genet* **16**, 8.

Fakouri, N. B., Hou, Y., Demarest, T. G., Christiansen, L. S., Okur, M. N., Mohanty, J. G., Croteau, D. L. and Bohr, V. A. (2019). Toward understanding genomic instability, mitochondrial dysfunction and aging. *Febs j* **286**, 1058-1073.

Fannin, S. W., Lesnefsky, E. J., Slabe, T. J., Hassan, M. O. and Hoppel, C. L. (1999). Aging selectivity decreases oxidative capacity in rat heart interfibrillar mitochondria. *Arch. Biochem. Biophys.* **372**, 399-407.

Feng, J., Bussière, F. and Hekimi, S. (2001). Mitochondrial electron transport is a key determinant of life span in *Caenorhabditis elegans*. *Dev Cell* **1**, 633-44.

Ferguson, M., Mockett, R. J., Shen, Y., Orr, W. C. and Sohal, R. S. (2005). Age-associated decline in mitochondrial respiration and electron transport in *Drosophila melanogaster*. *Biochem J* **390**, 501-11.

Ferrucci, L., Wilson, D. M., Donegà, S. and Gorospe, M. (2022). The energy–splicing resilience axis hypothesis of aging. *Nat. Research* **2**, 1-4.

Figueiredo, P. A., Powers, S. K., Ferreira, R. M., Appell, H. J. and Duarte, J. A. (2009). Aging impairs skeletal muscle mitochondrial bioenergetic function. *J. Gerontol. A. Biol. Sci. Med. Sci.* **64**, 21-33.

Finkel, T. (2015). The metabolic regulation of aging. *Nat Med* **21**, 1416-23.

Gäde, G. and Auerswald, L. (2002). Beetles' choice--proline for energy output: control by AKHs. *Comp. Biochem. Physiol. B Biochem. Mol. Biol.* **132**, 117-29.

Gemmell, N. J., Metcalf, V. J. and Allendorf, F. W. (2004). Mother's curse: the effect of mtDNA on individual fitness and population viability. *Trends Ecol Evol* **19**, 238-44.

Genova, M. L., Castelluccio, C., Fato, R., Parenti Castelli, G., Merlo Pich, M., Formiggini, G., Bovina, C., Marchetti, M. and Lenaz, G. (1995). Major changes in complex I activity in mitochondria from aged rats may not be detected by direct assay of NADH:coenzyme Q reductase. *Biochem. J.* **311**, 105-109.

Gnaiger, E. (2020). Mitochondrial pathways and respiratory control. An introduction to OXPHOS analysis. Innsbruck, Austria: Bioenerg. Commun.

Gnaiger, E., Kuznetsov, A. V., Schneeberger, S., Seiler, R., Brandacher, G., Steurer, W. and Margreiter, R. (2000). Mitochondria in the cold. In *Life in the cold*, eds. G. Heldmaier and M. Klingenspor), pp. 431-442. New York: Springer Berlin Heidelberg.

Graham, B. H., Waymire, K. G., Cottrell, B. A., Trounce, I. A., MacGregor, G. R. and Wallace, D. C. (1997). A mouse model for mitochondrial myopathy and cardiomyopathy resulting from a deficiency in the heart/muscle isoform of the adenine nucleotide translocator. *Nat. Genet.* **16**, 226-234.

Gruber, J., Ng, L. F., Fong, S., Wong, Y. T., Koh, S. A., Chen, C. B., Shui, G., Cheong, W. F., Schaffer, S., Wenk, M. R. et al. (2011). Mitochondrial changes in ageing *Caenorhabditis elegans*--what do we learn from superoxide dismutase knockouts? *PLOS ONE* **6**, e19444.

Guo, R., Zong, S., Wu, M., Gu, J. and Yang, M. (2017). Architecture of human mitochondrial respiratory megacomplex I(2)III(2)IV(2). *Cell* **170**, 1247-1257.e12.

Hamilton, B., Dong, Y., Shindo, M., Liu, W., Odell, I., Ruvkun, G. and Lee, S. S. (2005). A systematic RNAi screen for longevity genes in *C. elegans*. *Genes Dev* **19**, 1544-55.

Hancock, C. N., Liu, W., Alvord, W. G. and Phang, J. M. (2016). Co-regulation of mitochondrial respiration by proline dehydrogenase/oxidase and succinate. *Amino Acids* **48**, 859-872.

Hansen, M., Hsu, A. L., Dillin, A. and Kenyon, C. (2005). New genes tied to endocrine, metabolic, and dietary regulation of lifespan from a *Caenorhabditis elegans* genomic RNAi screen. *PLoS Genet* **1**, 119-28.

Hansford, R. G. (1978). Lipid oxidation by heart mitochondria from young adult and senescent rats. *Biochemical Journal* **170**, 285-295.

Haripriya, D., Devi, M. A., Kokilavani, V., Sangeetha, P. and Panneerselvam, C. (2004). Age-dependent alterations in mitochondrial enzymes in cortex, striatum and hippocampus of rat brain - potential role of L-Carnitine. *Biogerontology* **5**, 355-364.

Harman, D. (1956). Aging: A theory based on free radical and radiation chemistry. *J. Gerontol.* **11**, 298-300.

Harman, D. (1972). The biologic clock: the mitochondria? *J Am Geriatr Soc* **20**, 145-7.

Hekimi, S., Lapointe, J. and Wen, Y. (2011). Taking a "good" look at free radicals in the aging process. *Trends Cell Biol* **21**, 569-76.

Herrero, A. and Barja, G. (2000). Localization of the site of oxygen radical generation inside the complex I of heart and nonsynaptic brain mammalian mitochondria. *J Bioenerg Biomembr* **32**, 609-15.

Hirose, M., Schilf, P., Zarse, K., Busch, H., Fuellen, G., Jöhren, O., Köhling, R., König, I. R., Richer, B., Rupp, J. et al. (2019). Maternally inherited differences within mitochondrial complex I control murine healthspan. *Genes (Basel)* **10**.

Hoppel, C. L., Lesnefsky, E. J., Chen, Q. and Tandler, B. (2017). Mitochondrial dysfunction in cardiovascular aging. *Adv Exp Med Biol* **982**, 451-464.

Huang, J. and Lemire, B. D. (2009). Mutations in the *C. elegans* succinate dehydrogenase iron-sulfur subunit promote superoxide generation and premature aging. *J Mol Biol* **387**, 559-69.

Hwang, A. B. and Lee, S. J. (2011). Regulation of life span by mitochondrial respiration: the HIF-1 and ROS connection. *Aging (Albany NY)* **3**, 304-10.

Ichimiya, H., Huet, R. G., Hartman, P., Amino, H., Kita, K. and Ishii, N. (2002). Complex II inactivation is lethal in the nematode *Caenorhabditis elegans*. *Mitochondrion* **2**, 191-8.

Immonen, E., Rönn, J., Watson, C., Berger, D. and Arnqvist, G. (2016). Complex mitonuclear interactions and metabolic costs of mating in male seed beetles. *J Evol Biol* **29**, 360-70.

Ishii, N., Fujii, M., Hartman, P. S., Tsuda, M., Yasuda, K., Senoo-Matsuda, N., Yanase, S., Ayusawa, D. and Suzuki, K. (1998). A mutation in succinate dehydrogenase cytochrome b causes oxidative stress and ageing in nematodes. *Nature* **394**, 694-7.

Ishii, N., Takahashi, K., Tomita, S., Keino, T., Honda, S., Yoshino, K. and Suzuki, K. (1990). A methyl viologen-sensitive mutant of the nematode *Caenorhabditis elegans*. *Mutat Res* **237**, 165-71.

Itoh, K., Weis, S., Mehraein, P. and Müller-Höcker, J. (1996). Cytochrome *c* oxidase defects of the human substantia nigra in normal aging. *Neurobiol. Aging* **17**, 843-848.

Jang, S. and Javadov, S. (2018). Elucidating the contribution of ETC complexes I and II to the respirasome formation in cardiac mitochondria. *Sci Rep* **8**, 17732.

Jovanović, D., Dorđević, M., Savković, U. and Lazarević, J. (2014). The effect of mitochondrial complex I inhibitor on longevity of short-lived and long-lived seed beetles and its mitonuclear hybrids. *Biogerontology* **15**, 487-501.

Kayser, E. B., Morgan, P. G., Hoppel, C. L. and Sedensky, M. M. (2001). Mitochondrial expression and function of GAS-1 in *Caenorhabditis elegans*. *J. Biol. Chem.* **276**, 20551-20558.

Kayser, E. B., Sedensky, M. M. and Morgan, P. G. (2004). The effects of complex I function and oxidative damage on lifespan and anesthetic sensitivity in *Caenorhabditis elegans*. *Mech Ageing Dev* **125**, 455-64.

Kerner, J., Turkaly, P. J., Minkler, P. E. and Hoppel, C. L. (2001). Aging skeletal muscle mitochondria in the rat: decreased uncoupling protein-3 content. *Am. J. Physiol. Endocrin. Metab.* **281**, E1054-E1062.

Kirby, D. M., Crawford, M., Cleary, M. A., Dahl, H. H., Dennett, X. and Thorburn, D. R. (1999). Respiratory chain complex I deficiency: an underdiagnosed energy generation disorder. *Neurology* **52**, 1255-64.

Kirchman, P. A., Kim, S., Lai, C. Y. and Jazwinski, S. M. (1999). Interorganelle signaling is a determinant of longevity in Saccharomyces cerevisiae. *Genetics* **152**, 179-90.

Kirkwood, T. B. (2005). Understanding the odd science of aging. *Cell* **120**, 437-47.

Klaus, S. and Ost, M. (2020). Mitochondrial uncoupling and longevity - A role for mitokines? *Exp Gerontol* **130**, 110796.

Kleiber, M. (1961). The fire of life: An introduction to animal energetics.: John Wiley & Sons.

Kogot-Levin, A., Saada, A., Leibowitz, G., Soiferman, D., Douiev, L., Raz, I. and Weksler-Zangen, S. (2016). Upregulation of mitochondrial content in cytochrome *c* oxidase deficient fibroblasts. *PLOS ONE* **11**, e0165417.

Kowaltowski, A. J., de Souza-Pinto, N. C., Castilho, R. F. and Vercesi, A. E. (2009). Mitochondria and reactive oxygen species. *Free Radic. Biol. Med.* **47**, 333-343.

Kuang, J. and Ebert, P. R. (2012). The failure to extend lifespan via disruption of complex II is linked to preservation of dynamic control of energy metabolism. *Mitochondrion* **12**, 280-7.

Labbadia, J., Brielmann, R. M., Neto, M. F., Lin, Y. F., Haynes, C. M. and Morimoto, R. I. (2017). Mitochondrial stress restores the heat shock response and prevents proteostasis collapse during aging. *Cell Rep* **21**, 1481-1494.

Lakatos, A., Derbeneva, O., Younes, D., Keator, D., Bakken, T., Lvova, M., Brandon, M., Guffanti, G., Reglodi, D., Saykin, A. et al. (2010). Association between mitochondrial DNA variations and Alzheimer's disease in the ADNI cohort. *Neurobiol Aging* **31**, 1355-63.

Lakowski, B. and Hekimi, S. (1996). Determination of life-span in *Caenorhabditis elegans* by four clock genes. *Science* **272**, 1010-3.

Lambert, A. J. and Brand, M. D. (2004). Inhibitors of the quinone-binding site allow rapid superoxide production from mitochondrial NADH : ubiquinone oxidoreductase (complex I). *J. Biol. Chem.* **279**, 39414-39420.

Lambert, A. J., Buckingham, J. A., Boysen, H. M. and Brand, M. D. (2010). Low complex I content explains the low hydrogen peroxide production rate of heart mitochondria from the long-lived pigeon, *Columba livia*. *Aging Cell* **9**, 78-91.

Lane, S. J., Frankino, W. A., Elekonich, M. M. and Roberts, S. P. (2014). The effects of age and lifetime flight behavior on flight capacity in *Drosophila melanogaster*. *J Exp Biol* **217**, 1437-43.

Lanza, I. R., Befroy, D. E. and Kent-Braun, J. A. (2005). Age-related changes in ATP-producing pathways in human skeletal muscle *in vivo*. *J. Appl. Physiol.* **99**, 1736-1744.

Lapointe, J., Stepanyan, Z., Bigras, E. and Hekimi, S. (2009). Reversal of the mitochondrial phenotype and slow development of oxidative biomarkers of aging in long-lived Mclk1+/- mice. *J Biol Chem* **284**, 20364-74.

Larsen, S., Nielsen, J., Hansen, C. N., Nielsen, L. B., Wibrand, F., Stride, N., Schroder, H. D., Boushel, R., Helge, J. W., Dela, F. et al. (2012). Biomarkers of mitochondrial content in skeletal muscle of healthy young human subjects. *J. Physiol.* **590**, 3349-3360.

Lazarević, J., Dorđević, M., Stojković, B. and Tucić, N. (2013). Resistance to prooxidant agent paraquat in the short- and long-lived lines of the seed beetle (*Acanthoscelides obtectus*). *Biogerontology* **14**, 141-52.

Lazarevic, J., Tucic, N., Jovanovic, D. S., Vecera, J. and Kodrık, D. (2012). The effects of selection for early and late reproduction on metabolite pools in *Acanthoscelides obtectus* Say. *Insect Sci.* **19**, 303-314.

Le Bourg, E. and Minois, N. (1999). A mild stress, hypergravity exposure, postpones behavioral aging in *Drosophila melanogaster*. *Exp Gerontol* **34**, 157-72.

Lee, C. M., Aspnes, L. E., Chung, S. S., Weindruch, R. and Aiken, J. M. (1998). Influences of caloric restriction on age-associated skeletal muscle fiber characteristics and mitochondrial changes in rats and mice. *Ann. N. Y. Acad. Sci.* **854**, 182-191.

Lee, S. S., Lee, R. Y., Fraser, A. G., Kamath, R. S., Ahringer, J. and Ruvkun, G. (2003). A systematic RNAi screen identifies a critical role for mitochondria in *C. elegans* longevity. *Nat Genet* **33**, 40-8.

Lemieux, H. and Blier, P. U. (2022). Exploring thermal sensitivities and adaptations of oxidative phosphorylation pathways. *Metabolites* **12**, 1-20.

Lemieux, H., Blier, P. U. and Gnaiger, E. (2017). Remodeling pathway control of oxidative phosphorylation by temperature in the heart. *Sci. Rep.* **7**, 2840.

Lemieux, H. and Hoppel, C. L. (2009). Mitochondria in the human heart. *J. Bioenerg. Biomembr.* **41**, 99-106.

Lemieux, H., Semsroth, S., Antretter, H., Höfer, D. and Gnaiger, E. (2011). Mitochondrial respiratory control and early defects of oxidative phosphorylation in the failing human heart. *Int. J. Biochem. Cell. Biol.* **43**, 1729-1738.

Lemieux, H., Vazquez, E. J., Fujioka, H. and Hoppel, C. L. (2010). Decrease in mitochondrial function in rat cardiac permeabilized fibers correlates with the aging phenotype. *J. Gerontol. A. Biol. Sci. Med. Sci.* **65**, 1157-1164.

Lesnefsky, E. J., Gudz, T. I., Moghaddas, S., Migita, C. T., Ikeda-Saito, M., Trukaly, P. J. and Hoppel, C. L. (2001). Aging decreases electron transport complex III activity in heart interfibrillar mitochondria by alteration of the cytochrome *c* binding site. *J. Mol. Cell. Cardiol.* **33**, 37-47.

Lesnefsky, E. J., He, D., Moghaddas, S. and Hoppel, C. L. (2006). Reversal of mitochondrial defects before ischemia protects the aged heart. *FASEB J.* **20**, 1543-1545.

Lewis, K. N., Rubinstein, N. D. and Buffenstein, R. (2018). A window into extreme longevity; the circulating metabolomic signature of the naked mole-rat, a mammal that shows negligible senescence. *Geroscience* **40**, 105-121.

Li, Y., Wang, J., Xing, H. and Bao, J. (2022). Selenium mitigates ammonia-induced neurotoxicity by suppressing apoptosis, immune imbalance, and gut microbiota-driven metabolic disturbance in fattening pigs. *Biol Trace Elem Res*, 1-15.

Lin, A. L., Zhang, W., Gao, X. and Watts, L. (2015). Caloric restriction increases ketone bodies metabolism and preserves blood flow in aging brain. *Neurobiol Aging* **36**, 2296-2303.

Loeffen, J. L., Smeitink, J. A., Trijbels, J. M., Janssen, A. J., Triepels, R. H., Sengers, R. C. and van den Heuvel, L. P. (2000). Isolated complex I deficiency in children: clinical, biochemical and genetic aspects. *Hum. Mutat.* **15**, 123-34.

Long, Y. C., Tan, T. M., Takao, I. and Tang, B. L. (2014). The biochemistry and cell biology of aging: metabolic regulation through mitochondrial signaling. *Am J Physiol Endocrinol Metab* **306**, E581-91.

Longo, V. D. and Mattson, M. P. (2014). Fasting: molecular mechanisms and clinical applications. *Cell Metab* **19**, 181-92.

López-Otín, C., Blasco, M. A., Partridge, L., Serrano, M. and Kroemer, G. (2013). The hallmarks of aging. *Cell* **153**, 1194-217.

López-Otín, C., Galluzzi, L., Freije, J. M. P., Madeo, F. and Kroemer, G. (2016). Metabolic control of longevity. *Cell* **166**, 802-821.

Lu, B. and Guo, S. (2020). Mechanisms linking mitochondrial dysfunction and proteostasis failure. *Trends Cell Biol* **30**, 317-328.

Mansouri, A., Muller, F. L., Liu, Y., Ng, R., Faulkner, J., Hamilton, M., Richardson, A., Huang, T. T., Epstein, C. J. and Van Remmen, H. (2006). Alterations in mitochondrial function, hydrogen peroxide release and oxidative damage in mouse hind-limb skeletal muscle during aging. *Mech. Ageing Dev.* **127**, 298-306.

Martin, L. B., 2nd, Hasselquist, D. and Wikelski, M. (2006). Investment in immune defense is linked to pace of life in house sparrows. *Oecologia* **147**, 565-75.

Masoro, E. J. (2006). Dietary restriction-induced life extension: a broadly based biological phenomenon. *Biogerontology* **7**, 153-5.

Mast, H., Holody, C. and Lemieux, H. (2022). Fatty acid oxidation: A neglected factor in understanding the adjustment of mitochondrial function to cold temperatures. *J. Exp. Biol.*

Matarese, L. E. (1997). Indirect calorimetry: technical aspects. *J Am Diet Assoc* **97**, S154-60.

Mattson, M. P. and Arumugam, T. V. (2018). Hallmarks of brain aging: adaptive and pathological modification by metabolic states. *Cell Metab* **27**, 1176-1199.

Melvin, R. G. and Ballard, J. W. (2006). Intraspecific variation in survival and mitochondrial oxidative phosphorylation in wild-caught *Drosophila simulans*. *Aging Cell* **5**, 225-33.

Milani, M., Pihán, P. and Hetz, C. (2022). Mitochondria-associated niches in health and disease. *J Cell Sci* **135**.

Miller, M. S., Lekkas, P., Braddock, J. M., Farman, G. P., Ballif, B. A., Irving, T. C., Maughan, D. W. and Vigoreaux, J. O. (2008). Aging enhances indirect flight muscle fiber performance yet decreases flight ability in *Drosophila*. *Biophys J* **95**, 2391-401.

Minocherhomji, S., Tollefsbol, T. O. and Singh, K. K. (2012). Mitochondrial regulation of epigenetics and its role in human diseases. *Epigenetics* **7**, 326-34.

Minois, N. (2000). Longevity and aging: beneficial effects of exposure to mild stress. *Biogerontology* **1**, 15-29.

Miwa, S., Jow, H., Baty, K., Johnson, A., Czapiewski, R., Saretzki, G., Treumann, A. and von Zglinicki, T. (2014). Low abundance of the matrix arm of complex I in mitochondria predicts longevity in mice. *Nat Commun* **5**, 3837.

Morley, J. E., Baumgartner, R. N., Roubenoff, R., Mayer, J. and Nair, K. S. (2001). Sarcopenia. *J. Lab. Clin. Med.* **137**, 231-243.

Mukai, Y., Kamei, Y., Liu, X., Jiang, S., Sugimoto, Y., Mat Nanyan, N. S. B., Watanabe, D. and Takagi, H. (2019). Proline metabolism regulates replicative lifespan in the yeast Saccharomyces cerevisiae. *Microb Cell* **6**, 482-490.

Muller, F. L., Liu, Y., Abdul-Ghani, M. A., Lustgarten, M. S., Bhattacharya, A., Jang, Y. C. and Van Remmen, H. (2008). High rates of superoxide production in skeletal-muscle mitochondria respiring on both complex I- and complex II-linked substrates. *Biochem J* **409**, 491-9.

Munkácsy, E. and Rea, S. L. (2014). The paradox of mitochondrial dysfunction and extended longevity. *Exp Gerontol* **56**, 221-33.

Munro, D., Baldy, C., Pamenter, M. E. and Treberg, J. R. (2019). The exceptional longevity of the naked mole-rat may be explained by mitochondrial antioxidant defenses. *Aging Cell* **18**, e12916.

Munro, D., Pichaud, N., Paquin, F., Kemeid, V. and Blier, P. U. (2013). Low hydrogen peroxide production in mitochondria of the long-lived Arctica islandica: underlying mechanisms for slow aging. *Aging Cell.* **12**, 584-592.

Munro, D., Rodríguez, E. and Blier, P. U. (2023). The longest-lived metazoan, *Arctica islandica*, exhibits high mitochondrial H_2O_2 removal capacities. *Mitochondrion* **68**, 81-86.

Nagano, T., Nakashima, A., Onishi, K., Kawai, K., Awai, Y., Kinugasa, M., Iwasaki, T., Kikkawa, U. and Kamada, S. (2017). Proline dehydrogenase promotes senescence through the generation of reactive oxygen species. *J Cell Sci* **130**, 1413-1420.

Navarro, A. and Boveris, A. (2004). Rat brain and liver mitochondria develop oxidative stress and lose enzymatic activities on aging. *Am. J. Physiol. Regul. Integr. Comp. Physiol.* **287**, R1244-R1249.

Navarro, A., Gomez, C., López-Cepero, J. M. and Boveris, A. (2004). Beneficial effects of moderate exercise on mice aging: survival, behavior, oxidative stress, and mitochondrial electron transfer. *Am. J. Physiol. Regul. Integr. Comp. Physiol.* **286**, R505-R511.

Navarro, A., López-Cepero, J. M., Bández, M. J., Sánchez-Pino, M. J., Gómez, C., Cadenas, E. and Boveris, A. (2008). Hippocampal mitochondrial dysfunction in rat aging. *Am. J. Physiol. Regul. Integr. Comp. Physiol.* **294**, R501-R509.

Navarro, A., Sánchez-Pino, M. J., Gómez, C., Bández, M. J., Cadenas, E. and Boveris, A. (2007). Dietary thioproline decreases spontaneous food intake and increases survival and neurological function in mice. *Antioxid. Redox. Signal.* **9**, 131-141.

Neafsey, P. J. (1990). Longevity hormesis. A review. *Mech Ageing Dev* **51**, 1-31.

Niitepõld, K., Parry, H. A., Harris, N. R., Appel, A. G., de Roode, J. C., Kavazis, A. N. and Hood, W. R. (2022). Flying on empty: reduced mitochondrial function and flight capacity in food-deprived monarch butterflies. *J Exp Biol* **225**.

Nishimura, A., Yoshikawa, Y., Ichikawa, K., Takemoto, T., Tanahashi, R. and Takagi, H. (2021). Longevity regulation by proline oxidation in yeast. *Microorganisms* **9**, 1-11.

Ohkubo, E., Aida, K., Chen, J., Hayashi, J. I., Isobe, K., Tawata, M. and Onaya, T. (2000). A patient with type 2 diabetes mellitus associated with mutations in calcium sensing receptor gene and mitochondrial DNA. *Biochem Biophys Res Commun* **278**, 808-13.

Ojaimi, J., Masters, C. L., Opeskin, K., McKelvie, P. and Byrne, E. (1999). Mitochondrial respiratory chain activity in the human brain as a function of age. *Mech. Ageing Dev.* **111**, 39-47.

Okamoto, K. and Kondo-Okamoto, N. (2012). Mitochondria and autophagy: critical interplay between the two homeostats. *Biochim Biophys Acta* **1820**, 595-600.

Okatani, Y., Wakatsuki, A., Reiter, R. J. and Miyahara, Y. (2002). Hepatic mitochondrial dysfunction in senescence-accelerated mice: correction by long-term, orally administered physiological levels of melatonin. *J. Pineal. Res.* **33**, 127-133.

Owusu-Ansah, E., Song, W. and Perrimon, N. (2013). Muscle mitohormesis promotes longevity via systemic repression of insulin signaling. *Cell* **155**, 699-712.

Pamplona, R., Barja, G. and Portero-Otin, M. (2002). Membrane fatty acid unsaturation, protection against oxidative stress, and maximum life span - A homeoviscous-longevity adaptation? In *Increasing Healthy Life Span: Conventional Measures and Slowing the Innate Aging Process*, vol. 959, pp. 475-490. New York: New York Acad. Sciences.

Pang, S. and Curran, S. P. (2014). Adaptive capacity to bacterial diet modulates aging in *C. elegans*. *Cell Metab* **19**, 221-31.

Paradies, G., Ruggiero, F. M., Dinoi, P., Petrosillo, G. and Quagliariello, E. (1993). Decreased cytochrome oxidase activity and changes in phospholipids in heart mitochondria from hypothyroid rats. *Arch. Biochem. Biophys.* **307**, 91-95.

Paradies, G., Ruggiero, F. M., Petrosillo, G. and Quagliariello, E. (1994). Enhanced cytochrome oxidase activity and modification of lipids in heart mitochondria from hyperthyroid rats. *Biochimica and Biophysica Acta* **1225**, 165-170.

Paradies, G., Ruggiero, F. M., Petrosillo, G. and Quagliariello, E. (1997). Age-dependent decline in the cytochrome *c* oxidase activity in rat heart mitochondria: Role of cardiolipin. *FEBS Lett.* **406**, 136-138.

Pearl, R. (1928). The rate of living. London, UK: University of London Press.

Pérez, V. I., Van Remmen, H., Bokov, A., Epstein, C. J., Vijg, J. and Richardson, A. (2009). The overexpression of major antioxidant enzymes does not extend the lifespan of mice. *Aging Cell* **8**, 73-5.

Phillip, J. M., Aifuwa, I., Walston, J. and Wirtz, D. (2015). The mechanobiology of aging. *Annu Rev Biomed Eng* **17**, 113-141.

Picard, M., Taivassalo, T., Ritchie, D., Wright, K. J., Thomas, M. M., Romestaing, C. and Hepple, R. T. (2011). Mitochondrial structure and function are disrupted by standard isolation methods. *PLOS ONE* **6**, e18317.

Pujol, C., Bratic-Hench, I., Sumakovic, M., Hench, J., Mourier, A., Baumann, L., Pavlenko, V. and Trifunovic, A. (2013). Succinate dehydrogenase upregulation destabilize complex I and limits the lifespan of gas-1 mutant. *PLOS ONE* **8**, e59493.

Rasmussen, U. F., Krustrup, P., Kjaer, M. and Rasmussen, H. N. (2003a). Experimental evidence against the mitochondrial theory of aging - A study of isolated human skeletal muscle mitochondria. *Exp. Gerontol.* **38**, 877-886.

Rasmussen, U. F., Krustrup, P., Kjaer, M. and Rasmussen, H. N. (2003b). Human skeletal muscle mitochondrial metabolism in youth and senescence: no signs of functional changes in ATP formation and mitochondrial oxidative capacity. *Pflugers Arch.* **446**, 270-278.

Rattan, S. I. (2000). Ageing, gerontogenes, and hormesis. *Indian J Exp Biol* **38**, 1-5.

Rattan, S. I. (2001). Applying hormesis in aging research and therapy. *Hum Exp Toxicol* **20**, 281-5; discussion 293-4.

Rattan, S. I. (2004). Aging, anti-aging, and hormesis. *Mech Ageing Dev* **125**, 285-9.

Rauthan, M., Ranji, P., Abukar, R. and Pilon, M. (2015). A mutation in *Caenorhabditis elegans* NDUF-7 activates the mitochondrial stress response and prolongs lifespan via ROS and CED-4. *G3 (Bethesda)* **5**, 1639-48.

Rea, S. L., Ventura, N. and Johnson, T. E. (2007). Relationship between mitochondrial electron transport chain dysfunction, development, and life extension in *Caenorhabditis elegans*. *PLoS Biol* **5**, e259.

Réale, D., Garant, D., Humphries, M. M., Bergeron, P., Careau, V. and Montiglio, P. O. (2010). Personality and the emergence of the pace-of-life syndrome concept at the population level. *Philos Trans R Soc Lond B Biol Sci* **365**, 4051-63.

Rehman, M. U., Sehar, N., Dar, N. J., Khan, A., Arafah, A., Rashid, S., Rashid, S. M. and Ganaie, M. A. (2023). Mitochondrial dysfunctions, oxidative stress and neuroinflammation as therapeutic targets for neurodegenerative diseases: An update on current advances and impediments. *Neurosci Biobehav Rev* **144**, 104961.

Ricklefs, R. E. and Wikelski, M. (2002). The physiology/life-history nexus. *Trends Ecol. Evol.* **17**, 462-468.

Ristow, M. (2014). Unraveling the truth about antioxidants: mitohormesis explains ROS-induced health benefits. *Nat Med* **20**, 709-11.

Ristow, M. and Schmeisser, K. (2014). Mitohormesis: Promoting health and lifespan by increased levels of reactive oxygen species (ROS). *Dose Response* **12**, 288-341.

Ristow, M. and Zarse, K. (2010). How increased oxidative stress promotes longevity and metabolic health: The concept of mitochondrial hormesis (mitohormesis). *Exp Gerontol* **45**, 410-8.

Rodríguez, E., Hakkou, M., Hagen, T. M., Lemieux, H. and Blier, P. U. (2021). Divergences in the control of mitochondrial respiration are associated with life-span variation in marine bivalves. *J. Gerontol. A Biol. Med. Sci.* **76**, 796-804.

Rodríguez, E., Radke, A., Hagen, T. M. and Blier, P. U. (2022). Supercomplex organization of the electron transfer system in marine bivalves, a model of extreme longevity. *J Gerontol A Biol Sci Med Sci* **77**, 283-290.

Rouland, C., Brauman, A., Labat, M. and Lepage, M. (1993). Nutritional factors affecting methane emission from termites. *Chemosphere* **26**, 617-622.

Rustin, P., Lebidois, J., Chretien, D., Bourgeron, T., Piechaud, J. F., Rötig, A., Sidi, D. and Munnich, A. (1993). The investigation of respiratory chain disorders in heart using endomyocardial biopsies. *J Inherit Metab Dis* **16**, 541-4.

Schaar, C. E., Dues, D. J., Spielbauer, K. K., Machiela, E., Cooper, J. F., Senchuk, M., Hekimi, S. and Van Raamsdonk, J. M. (2015). Mitochondrial and cytoplasmic ROS have opposing effects on lifespan. *PLoS Genet* **11**, e1004972.

Schiavi, A. and Ventura, N. (2014). The interplay between mitochondria and autophagy and its role in the aging process. *Exp Gerontol* **56**, 147-53.

Schmauck-Medina, T., Molière, A., Lautrup, S., Zhang, J., Chlopicki, S., Madsen, H. B., Cao, S., Soendenbroe, C., Mansell, E., Vestergaard, M. B. et al. (2022). New hallmarks of ageing: a 2022 Copenhagen ageing meeting summary. *Aging (Albany NY)* **14**, 6829-6839.

Schulz, T. J., Zarse, K., Voigt, A., Urban, N., Birringer, M. and Ristow, M. (2007). Glucose restriction extends *Caenorhabditis elegans* life span by inducing mitochondrial respiration and increasing oxidative stress. *Cell Metab* **6**, 280-93.

Schutz, Y. and Ravussin, E. (1980). Respiratory quotients lower than 0.70 in ketogenic diets. *Am J Clin Nutr* **33**, 1317-9.

Scott, K. Y., Matthew, R., Woolcock, J., Silva, M. and Lemieux, H. (2019). Adjustments in control of mitochondrial respiratory capacity to tolerate temperature fluctuations. *J. Exp. Biol.* **222**, 1-11.

Sedensky, M. M. and Morgan, P. G. (2006). Mitochondrial respiration and reactive oxygen species in *C. elegans*. *Exp. Gerontol.* **41**, 957-967.

Seslija, D., Blagojević, D., Spasić, M. and Tucić, N. (1999). Activity of superoxide dismutase and catalase in the bean weevil (*Acanthoscelides obtectus*) selected for postponed senescence. *Exp Gerontol* **34**, 185-95.

Seslija, D., Lazarevic, J., Jankovic, B. and Tucic, N. (2009). Mating behavior in the seed beetle *Acanthoscelides obtectus* selected for early and late reproduction. *Behav. Ecol.* **20**, 547-552.

Short, K. R., Bigelow, M. L., Kahl, J., Singh, R., Coenen-Schimke, J., Raghavakaimal, S. and Nair, K. S. (2005). Decline in skeletal muscle mitochondrial function with aging in humans. *Proc. Natl. Acad. Sci. U.S.A.* **102**, 5618-5623.

Simon, A. F., Liang, D. T. and Krantz, D. E. (2006). Differential decline in behavioral performance of *Drosophila melanogaster* with age. *Mech Ageing Dev* **127**, 647-51.

Son, J. M. and Lee, C. (2019). Mitochondria: multifaceted regulators of aging. *BMB Rep* **52**, 13-23.

Srere, P. A. (1969). Citrate synthase. *Methods Enzymol.* **13**, 3-11.

Srivastava, S. (2017). The mitochondrial basis of aging and age-related disorders. *Genes (Basel)* **8**.

St-Pierre, J., Buckingham, J. A., Roebuck, S. J. and Brand, M. D. (2002). Topology of superoxide production from different sites in the mitochondrial electron transport chain. *J. Biol. Chem.* **277**, 44784-90.

Stojković, B. and Savković, U. (2011). Gender differences in longevity in early and late reproduced lines of the seed beetle. *Arch. Biol. Sci. Belgrade* **63**, 129-136.

Stojkovic, B., Seslija Jovanovic, D., Tucic, B. and Tucic, N. (2010). Homosexual behaviour and its longevity cost in females and males of the seed beetle *Acanthoscelides obtectus*. *Physiol. Entomol.* **35**, 308-316.

Stuart, J. A., Maddalena, L. A., Merilovich, M. and Robb, E. L. (2014). A midlife crisis for the mitochondrial free radical theory of aging. *Longev Healthspan* **3**, 4.

Sugiyama, S., Takasawa, M., Hayakawa, M. and Ozawa, T. (1993). Changes in skeletal muscle, heart and liver mitochondrial electron transport activities in rats and dogs of various ages. *Biochem. Mol. Biol. Int.* **30**, 937-944.

Sun, N., Youle, R. J. and Finkel, T. (2016). The mitochondrial basis of aging. *Mol Cell* **61**, 654-666.

Sural, S., Liang, C. Y., Wang, F. Y., Ching, T. T. and Hsu, A. L. (2020). HSB-1/HSF-1 pathway modulates histone H4 in mitochondria to control mtDNA transcription and longevity. *Sci Adv* **6**.

Suthammarak, W., Yang, Y. Y., Morgan, P. G. and Sedensky, M. M. (2009). Complex I function is defective in complex IV-deficient *Caenorhabditis elegans*. *J Biol Chem* **284**, 6425-35.

Szeto, S. S. W., Reinke, S. N., Sykes, B. D. and Lemire, B. D. (2007). Ubiquinone-binding site mutations in the Saccharomyces cerevisiae succinate dehydrogenase generate superoxide and lead to the accumulation of succinate. *J Biol Chem* **282**, 27518-27526.

Tapia, P. C. (2006). Sublethal mitochondrial stress with an attendant stoichiometric augmentation of reactive oxygen species may precipitate many of the beneficial alterations in cellular physiology produced by caloric restriction, intermittent fasting, exercise and dietary phytonutrients: "Mitohormesis" for health and vitality. *Med Hypotheses* **66**, 832-43.

Teulier, L., Weber, J. M., Crevier, J. and Darveau, C. A. (2016). Proline as a fuel for insect flight: enhancing carbohydrate oxidation in hymenopterans. *Proc. Biol. Sci.* **283**, 1-8.

Tian, L., Cai, Q. and Wei, H. (1998). Alterations of antioxidant enzymes and oxidative damage to macromolecules in different organs of rats during aging. *Free Radic. Biol. Med.* **24**, 1477-1484.

Tian, Y., Garcia, G., Bian, Q., Steffen, K. K., Joe, L., Wolff, S., Meyer, B. J. and Dillin, A. (2016). Mitochondrial stress induces chromatin reorganization to promote longevity and UPR(mt). *Cell* **165**, 1197-1208.

Tofilski, A. (2000). Senescence and learning in honeybee (Apis mellifera) workers. *Acta Neurobiol Exp (Wars)* **60**, 35-9.

Tomtheelnganbee, E., Sah, P. and Sharma, R. (2022). Mitochondrial function and nutrient sensing pathways in ageing: enhancing longevity through dietary interventions. *Biogerontology* **23**, 657-680.

Tonkonogi, M., Fernström, M., Walsh, B., Ji, L. L., Rooyackers, O., Hammarqvist, F., Wernerman, J. and Sahlin, K. (2003). Reduced oxidative power but unchanged antioxidative capacity in skeletal muscle from aged humans. *Pflugers Arch.* **446**, 261-269.

Torres, C. A. and Perez, V. I. (2008). Proteasome modulates mitochondrial function during cellular senescence. *Free Radic Biol Med* **44**, 403-14.

Tucić, N., Gliksman, I., Šešlija, D., Milanović, D., Mikuljanac, S. and Stojković, O. (1996). Laboratory evolution of longevity in the bean weevil (*Acanthoscelides obtectus*). *J. Evol. Biol.* **9**, 485-503.

Tucić, N., Stojković, O., Gliksman, I., Milanović, A. and Šešlija, D. (1997). Laboratory evolution of life-history traits in the bean weevil (*Acanthoscelides obtectus*): The effects of density-dependent and age-specific selection. *Evolution* **51**, 1896-1909.

Ukhueduan, B., Schumpert, C., Kim, E., Dudycha, J. L. and Patel, R. C. (2022). Relationship between oxidative stress and lifespan in Daphnia pulex. *Sci Rep* **12**, 2354.

van der Walt, J. M., Nicodemus, K. K., Martin, E. R., Scott, W. K., Nance, M. A., Watts, R. L., Hubble, J. P., Haines, J. L., Koller, W. C., Lyons, K. et al. (2003). Mitochondrial polymorphisms significantly reduce the risk of Parkinson disease. *Am J Hum Genet* **72**, 804-11.

Van Raamsdonk, J. M. and Hekimi, S. (2009). Deletion of the mitochondrial superoxide dismutase sod-2 extends lifespan in *Caenorhabditis elegans*. *PLoS Genet* **5**, e1000361.

Vazquez, E. J. and Hoppel, C. L. (2004). Aging decreases the activity of complex III in rat hepatic mitochondria. *FASEB J.* **18**.

Vazquez, E. J. and Hoppel, C. L. (2005). Aging decreases mitochondrial electron transport at complex III. *FASEB J.* **19**.

Veech, R. L., Bradshaw, P. C., Clarke, K., Curtis, W., Pawlosky, R. and King, M. T. (2017). Ketone bodies mimic the life span extending properties of caloric restriction. *IUBMB Life* **69**, 305-314.

Verbeke, P., Clark, B. F. and Rattan, S. I. (2000). Modulating cellular aging in vitro: hormetic effects of repeated mild heat stress on protein oxidation and glycation. *Exp Gerontol* **35**, 787-94.

Viltard, M., Durand, S., Pérez-Lanzón, M., Aprahamian, F., Lefevre, D., Leroy, C., Madeo, F., Kroemer, G. and Friedlander, G. (2019). The metabolomic signature of extreme longevity: naked mole rats versus mice. *Aging (Albany NY)* **11**, 4783-4800.

Vogt, J. T. and Appel, A. G. (1999). Standard metabolic rate of the fire ant, Solenopsis invicta Buren: effects of temperature, mass, and caste. *J Insect Physiol* **45**, 655-666.

Walker, D. W., Hájek, P., Muffat, J., Knoepfle, D., Cornelison, S., Attardi, G. and Benzer, S. (2006). Hypersensitivity to oxygen and shortened lifespan in a *Drosophila* mitochondrial complex II mutant. *Proc Natl Acad Sci U S A* **103**, 16382-7.

Wallace, D. C. (2005). A mitochondrial paradigm of metabolic and degenerative diseases, aging, and cancer: a dawn for evolutionary medicine. *Annu Rev Genet* **39**, 359-407.

Wan, Y. and Finkel, T. (2020). The mitochondria regulation of stem cell aging. *Mech Ageing Dev* **191**, 111334.

Wang, A., Mouser, J., Pitt, J., Promislow, D. and Kaeberlein, M. (2016). Rapamycin enhances survival in a *Drosophila* model of mitochondrial disease. *Oncotarget* **7**, 80131-80139.

Wightman, J. A. (1978). The ecology of *Callosobruchus analis* (Coleoptera: Bruchidae): Energetics and energy reserves of the adults. *J. Anim. Ecol.* **47**, 131-142.

Wikelski, M., Spinney, L., Schelsky, W., Scheuerlein, A. and Gwinner, E. (2003). Slow pace of life in tropical sedentary birds: a common-garden experiment on four stonechat populations from different latitudes. *Proc Biol Sci* **270**, 2383-8.

Wong, A., Boutis, P. and Hekimi, S. (1995). Mutations in the clk-1 gene of *Caenorhabditis elegans* affect developmental and behavioral timing. *Genetics* **139**, 1247-59.

Wu, Z., Senchuk, M. M., Dues, D. J., Johnson, B. K., Cooper, J. F., Lew, L., Machiela, E., Schaar, C. E., DeJonge, H., Blackwell, T. K. et al. (2018). Mitochondrial unfolded protein response transcription factor ATFS-1 promotes longevity in a long-lived mitochondrial mutant through activation of stress response pathways. *BMC Biol* **16**, 147.

Xin, N., Durieux, J., Yang, C., Wolff, S., Kim, H. E. and Dillin, A. (2022). The UPRmt preserves mitochondrial import to extend lifespan. *J Cell Biol* **221**.

Xu, C., Hwang, W., Jeong, D. E., Ryu, Y., Ha, C. M., Lee, S. V., Liu, L. and He, Z. M. (2018). Genetic inhibition of an ATP synthase subunit extends lifespan in *C. elegans*. *Sci Rep* **8**, 14836.

Yamamori, T., Yasui, H., Yamazumi, M., Wada, Y., Nakamura, Y., Nakamura, H. and Inanami, O. (2012). Ionizing radiation induces mitochondrial reactive oxygen species production accompanied by upregulation of mitochondrial electron transport chain function and mitochondrial content under control of the cell cycle checkpoint. *Free Radical Biology and Medicine* **53**, 260-270.

Yang, W. and Hekimi, S. (2010a). A mitochondrial superoxide signal triggers increased longevity in *Caenorhabditis elegans*. *PLoS Biol* **8**, e1000556.

Yang, W. and Hekimi, S. (2010b). Two modes of mitochondrial dysfunction lead independently to lifespan extension in *Caenorhabditis elegans*. *Aging Cell* **9**, 433-47.

Yang, W., Li, J. and Hekimi, S. (2007). A measurable increase in oxidative damage due to reduction in superoxide detoxification fails to shorten the life span of long-lived mitochondrial mutants of *Caenorhabditis elegans*. *Genetics* **177**, 2063-74.

Yasuda, K., Ishii, T., Suda, H., Akatsuka, A., Hartman, P. S., Goto, S., Miyazawa, M. and Ishii, N. (2006). Age-related changes of mitochondrial structure and function in *Caenorhabditis elegans*. *Mech Ageing Dev* **127**, 763-70.

Yun, J. and Finkel, T. (2014). Mitohormesis. *Cell Metab* **19**, 757-66.

Zheng, Q., Huang, J. and Wang, G. (2019). Mitochondria, telomeres and telomerase subunits. *Front Cell Dev Biol* **7**, 274.

Zid, B. M., Rogers, A. N., Katewa, S. D., Vargas, M. A., Kolipinski, M. C., Lu, T. A., Benzer, S. and Kapahi, P. (2009). 4E-BP extends lifespan upon dietary restriction by enhancing mitochondrial activity in *Drosophila*. *Cell* **139**, 149-60.

Zieliński, P., Smith, A. C., Smith, A. G. and Robinson, A. J. (2016). Metabolic flexibility of mitochondrial respiratory chain disorders predicted by computer modelling. *Mitochondrion* **31**, 45-55.